NASA/TM—2000-210576

Fatigue Characterization of Alloy 10: A 1300F Disk Alloy for Small Gas Turbine Engines

John Gayda
Glenn Research Center, Cleveland, Ohio

November 2000

The NASA STI Program Office . . . in Profile

Since its founding, NASA has been dedicated to the advancement of aeronautics and space science. The NASA Scientific and Technical Information (STI) Program Office plays a key part in helping NASA maintain this important role.

The NASA STI Program Office is operated by Langley Research Center, the Lead Center for NASA's scientific and technical information. The NASA STI Program Office provides access to the NASA STI Database, the largest collection of aeronautical and space science STI in the world. The Program Office is also NASA's institutional mechanism for disseminating the results of its research and development activities. These results are published by NASA in the NASA STI Report Series, which includes the following report types:

- TECHNICAL PUBLICATION. Reports of completed research or a major significant phase of research that present the results of NASA programs and include extensive data or theoretical analysis. Includes compilations of significant scientific and technical data and information deemed to be of continuing reference value. NASA's counterpart of peer-reviewed formal professional papers but has less stringent limitations on manuscript length and extent of graphic presentations.

- TECHNICAL MEMORANDUM. Scientific and technical findings that are preliminary or of specialized interest, e.g., quick release reports, working papers, and bibliographies that contain minimal annotation. Does not contain extensive analysis.

- CONTRACTOR REPORT. Scientific and technical findings by NASA-sponsored contractors and grantees.

- CONFERENCE PUBLICATION. Collected papers from scientific and technical conferences, symposia, seminars, or other meetings sponsored or cosponsored by NASA.

- SPECIAL PUBLICATION. Scientific, technical, or historical information from NASA programs, projects, and missions, often concerned with subjects having substantial public interest.

- TECHNICAL TRANSLATION. English-language translations of foreign scientific and technical material pertinent to NASA's mission.

Specialized services that complement the STI Program Office's diverse offerings include creating custom thesauri, building customized data bases, organizing and publishing research results . . . even providing videos.

For more information about the NASA STI Program Office, see the following:

- Access the NASA STI Program Home Page at ***http://www.sti.nasa.gov***

- E-mail your question via the Internet to help@sti.nasa.gov

- Fax your question to the NASA Access Help Desk at 301–621–0134

- Telephone the NASA Access Help Desk at 301–621–0390

- Write to:
  NASA Access Help Desk
  NASA Center for AeroSpace Information
  7121 Standard Drive
  Hanover, MD 21076

NASA/TM—2000-210576

Fatigue Characterization of Alloy 10: A 1300F Disk Alloy for Small Gas Turbine Engines

John Gayda
Glenn Research Center, Cleveland, Ohio

National Aeronautics and
Space Administration

Glenn Research Center

November 2000

Trade names or manufacturers' names are used in this report for identification only. This usage does not constitute an official endorsement, either expressed or implied, by the National Aeronautics and Space Administration.

Available from

NASA Center for Aerospace Information
7121 Standard Drive
Hanover, MD 21076
Price Code: A03

National Technical Information Service
5285 Port Royal Road
Springfield, VA 22100
Price Code: A03

Available electronically at http://gltrs.grc.nasa.gov/GLTRS

INTRODUCTION

Gas turbine engines for future subsonic engines will probably have higher pressure ratios which require nickel-base superalloy disks with 1300F temperature capability. To help fulfill this need NASA's AST Disk Program was initiated to develop manufacturing technologies for advanced disk alloys. In that program GEAE and PWA focused their attention on a large engine disk alloy developed under NASA's HSR Program, while Honeywell and Allison opted to focus their attention on Alloy 10, a high strength nickel-base disk alloy, developed by Honeywell for application in smaller gas turbine engines. Eight heat treat options for Alloy 10 were studied by Honeywell and Allison. The study was designed to evaluate the effect of solution temperature, cooling rate, and stabilization on key mechanical properties for disk application. After screening the results, Honeywell, Allison, and NASA selected the B1 (subsolvus, fan-cooled, and direct age) heat treatment for extensive fatigue characterization, under NASA's Ultrasafe Program, as it was deemed to have the best balance of properties and the lowest cost for near term application.

In this paper, the fatigue characterization of the B1 heat treatment for Alloy 10 is presented. Both smooth fatigue data, at varying R-ratios, as well as notch fatigue data at representative bore and rim temperatures were evaluated. Analysis of the fatigue data using the Smith-Watson-Topper approach and finite element analysis of the notch fatigue specimen was employed to help understand material behavior. In addition, tensile, creep, and crack growth data of the B1 heat treatment are reviewed for completeness.

MATERIAL & PROCEDURES

Alloy 10 is a high strength nickel-base superalloy, with a gamma prime content of about 55%. Its composition is shown in Table 1. Due to the alloy's high gamma prime content it is produced by powder metallurgy. In this study, argon atomized powder was produced from remelt stock by Special Metals Corporation which was subsequently screened to –270 mesh, canned, and hot isostatically pressed (HIP) at 2000F and 15KSI for 3 hours. The HIP billet was then extruded at 2025F using a 6:1 extrusion ratio. After sonic inspection, mults were cut from the extrusion and isothermally forged into "pancake" shapes about 14" in diameter and 2" thick by Wyman-Gordon. The B1 forging was then given a subsolvus solution at 2125F/2.5Hr and fan cooled resulting in an 11.8 ASTM grain size and a porosity level less than 0.1% as shown in Figure 1. This was followed by an aging cycle at 1400F/16Hr. More details on the exact processing history can be found in Reference 1.

Isothermal fatigue tests were run at 750F and 1300F to simulate bore and rim conditions respectively. Smooth fatigue testing was run under axial strain control with R-ratios of –1, 0.0, and 0.6, while notch fatigue testing (Kt=2) was run under load control with an R-ratio of 0.0. The test frequency for all fatigue tests was 0.3Hz for the first 24 hours and 5Hz thereafter. After 24 hours the smooth fatigue tests were restarted in load control using the stabilized peak loads established under strain control. The smooth fatigue bars had a 0.250" diameter by 0.6" long gage section and the notch fatigue bars had a 0.250"

diameter at the root of the v-notch as shown in Figure 2. All fatigue tests were run in air to failure.

RESULTS & DISCUSSION

Monotonic Properties. Tensile and creep properties for Alloy 10 were run under the AST Program, Reference 1, and are reviewed below for the B1 heat treatment. Tensile data was generated from room temperature through 1500F. The modulus, strength, and elongation are plotted against temperature in Figures 3 through 5. Examination of the data clearly shows a significant drop in modulus, strength, and elongation between 750F and 1300F. Creep data on the B1 heat treatment is presented using a Larson-Miller format in Figure 6. At 750F there is little if any creep below the yield strength, however, at 1300F a stress level of 100KSI, significantly less than the yield strength, produces 0.2% creep strain in about 400 hours. The tensile and creep properties of Alloy 10 with the B1 heat treatment are generally better than that of current generation, fine grain disk alloys.

Crack Growth. Crack growth data using a small, surface flaw specimen was generated on Alloy 10 under an earlier Ultrasafe task, Reference 2. The data for the B1 heat treatment are reviewed below. Figure 7 shows crack growth rates are about one order of magnitude faster at 1300F than 750F. Further, imposing a dwell at peak load produces a significant acceleration of crack growth at 1300F. This is a serious shortcoming for any of the fine grain microstructures, including the B1 heat treatment. Relative to other fine grain disk alloys, the crack growth rate of Alloy 10 with the B1 heat treatment is generally comparable to current generation disk alloys.

Smooth Bar Fatigue Tests. The cyclic stress-strain response of Alloy 10 with the B1 heat treatment was found to be relatively stable for fatigue tests at 750F or 1300F. Further, differences in R-ratio, $strain_{max}/strain_{min}$, appeared to have little impact on cyclic stress-strain response at half life as seen in Figures 8 and 9. As modulus and yield strength vary with test temperature, it is not surprising to find that the stress range is significantly greater at 750F than 1300F for a given strain. This is especially evident at the highest strain ranges. Unlike stress range, max stress was found to have a significant R-ratio dependence. Figures 10 and 11 show lower R-ratios give rise to lower max stress values at either test temperature, however, the data tends to converge at higher strain ranges at either temperature. Comparing max stress values at 750F and 1300F, it is clear that max stress levels are consistently higher at 750F for a given R-ratio and strain range, as one might expect.

Strain range versus fatigue life data at 750F and 1300F, Figure 12 and 13 respectively, were found to have a strong R-ratio dependence at low strains, but at higher strains the R-ratio dependence diminished. In general, a higher R-ratio produced shorter lives for a given strain range. This result is probably related to the max stress, which also increases with R-ratio. These observations suggest that fatigue data may collapse along a single curve if life is plotted against some function of max stress and strain range at either

temperature. The Smith-Watson-Topper approach, Reference 3, yields a parameter, SWT, by combining max stress and strain range as follows:

$$SWT=(Modulus*Stress_{max}*Strain_{range}/2)^{0.5}$$

Figure 14 and 15 show the results of plotting SWT versus fatigue life at 750F and 1300F respectively. The data fit is greatly improved compared to the strain range versus fatigue life plots at either temperature. Comparison of fatigue life at 750F and 1300F is now much simpler, and, as shown in Figure 16, one sees the lower temperature fatigue lives are significantly longer for a given SWT value.

Notch Fatigue Tests. Life data for notch fatigue tests are presented in Figures 17 and 18 at 750F and 1300F respectively. In these plots, fatigue life of Alloy 10 with the B1 heat treatment is plotted against the nominal maximum stress at the notch root, i.e. load divided by area at the notch root. For comparative purposes a limited number of load controlled fatigue tests were also run on smooth bars (Kt=1) to illustrate the deleterious effect of the notch. Temperature has a dramatic impact on the notch fatigue life as seen in Figure 19. At high stresses the 750F life is much longer, which is undoubtedly related to differences in alloy strength at the two test temperatures. However, at low stresses the data converge. This trend may result from creep/relaxation effects at 1300F. To gain a quantitative understanding of these issues a detailed stress analysis of the notch root was pursued.

A 2-D axisymmetric finite element stress analysis of the notch root was run to quantify evolution of the stress state during the fatigue tests. The analysis was run at two stress levels, 100KSI and 140KSI, and both test temperatures. A bilinear stress-strain behavior was employed to describe deformation response assuming a plastic modulus of 2000KSI. At 750F, an isotropic hardening model was selected with a 29000KSI modulus and a yield strength of 170KSI. At 1300F, a viscoplastic model was selected with a 26000KSI modulus, a yield strength of 160KSI, and a power law creep function based on the relaxation data shown in Figure 20.

The analysis at 750F was relatively simple as the stress state stabilized within a few cycles. For the 100KSI notch fatigue test, the axial stresses exceeded 200KSI at peak load as shown in Figure 21. Upon unloading, the axial stresses became compressive at the root of the notch as shown in Figure 22. For the 140KSI notch fatigue test, the axial stresses at the root of the notch ran about 240KSI at peak load and –75KSI upon unloading. As the stress state is multiaxial, both the axial and effective stress was monitored to determine the point at which the stress state stabilized. As previously stated, this occurred within a few cycles at 750F and is documented in tabular form in the appendix. A complete listing of all stabilized stresses and strains are also tabulated in the appendix.

The analysis at 1300F was more complex as the stress state could take many hundreds or thousands of cycles to stabilize since the material can creep/relax. As it would be impractical to run the finite element analysis using the exact waveform, an approximation of the cyclic nature for this problem was required. To this end the loading waveform

shown in Figure 23 was employed. Note that the time for each cycle was increased to 2000 seconds per cycle at 140KSI and 20000 seconds for 100KSI. To approximate real time effects on the first cycle, creep was zeroed leaving time-independent plasticity behavior as the only source of inelastic response. Creep effects were then introduced on the second cycle, starting at zero and ramping linearly to full effect at the end of the cycle. The analyses were continued to the approximate run times for real tests and the results are tabulated in the appendix using the same format as the data at 750F. The evolution of the stress state, measured by the Von Mises stress, is presented in Figures 24 and 25. Very little change in the peak stress is noted in the 140KSI notch fatigue tests at 1300F, however, in the 100KSI notch fatigue test there is a rather significant decay in the peak stress at 1300F. This is a direct result of the variation in test duration experimentally, and cycle period analytically, between the two conditions.

Using the results of the finite element analysis and the Smith-Watson-Topper expression, predictions of notch fatigue life were made. First, values of max stress and strain range at the half life were obtained from the element at the notch root. Then a value of SWT was computed and a life estimate was obtained from the appropriate smooth bar fatigue plot in Figure 16. In the first attempt, axial values of stress and strain were employed, which are nearly equivalent to the principal stress and strain values that have been employed in multiaxial fatigue problems, Reference 4. However, the predictions were extremely conservative. A second attempt, using effective values of stress and strain were tried, and the match with experimental data was significantly better. These results are presented in Figure 26. Although the predictions still tend to be conservative, they do reflect the trends observed in the experimental data. This analysis tends to confirm the proposition which attributes differences in notch fatigue life at the two test temperatures to changes in alloy strength at high stresses, and the increased importance of creep/relaxation at lower stresses.

SUMMARY & CONCLUSIONS

A detailed fatigue characterization of Alloy 10, a high strength nickel-based disk alloy, was conducted on test coupons machined from a "pancake" forging. Smooth bar, strain controlled fatigue testing at various R-ratios was run at representative bore, 750F, and rim, 1300F, temperatures. This was followed by notch fatigue testing (Kt=2) run under load control. Analysis of the fatigue data using a Smith-Watson-Topper approach and finite element analysis of the notch root was employed to understand material behavior in these tests.

Smooth bar fatigue data showed a significant R-ratio dependence at either test temperature which could be accounted for using a Smith-Watson-Topper parameter, SWT. In general, fatigue life was longer at 750F than 1300F for a given SWT. For notch fatigue tests, life was longer at 750F than 1300F but only at higher stresses. This was attributed to differences in alloy strength. At lower stresses, finite element analysis suggested that convergence of fatigue life at both temperatures resulted from relaxation of stresses at the notch root in the 1300F tests.

REFERENCES

1. Jain, S. K., Regional Engine Disk Process Development Final Report, NASA Contract NAS3-27720 Task 4.2.4, September 1999.
2. Telesman, J., Kantzos, P., and Gayda, J., Ultrasafe Crack Growth Data, In Preparation.
3. Smith, K. N., Watson, P., and Topper, T. H., A Stress-Strain Function for the Fatigue of Metal, Journal of Materials, Vol. 5, No. 4, December 1970, pp. 767-778.
4. Socie, D., Multiaxial Fatigue Damage Models, Journal of Engineering Materials and Technology, Vol. 109, October 1987, pp. 293-298.

TABLE 1. COMPOSITION OF ALLOY 10 IN W/O.

Cr	Co	Al	Ti	Nb	Mo	W	Ta	C	B	Zr	Ni
10.2	14.9	3.69	3.93	1.87	2.73	6.2	0.9	0.03	0.03	0.10	Bal

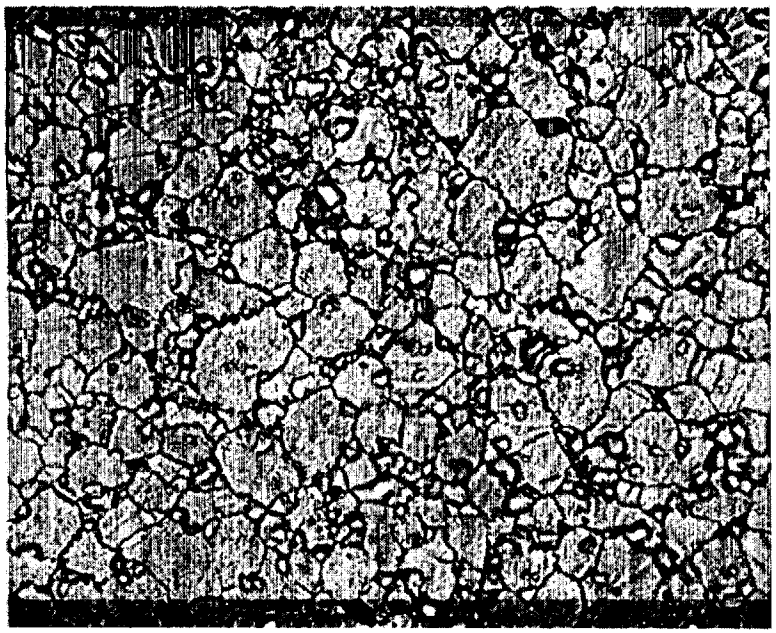

ASTM Grain Size = 11.8

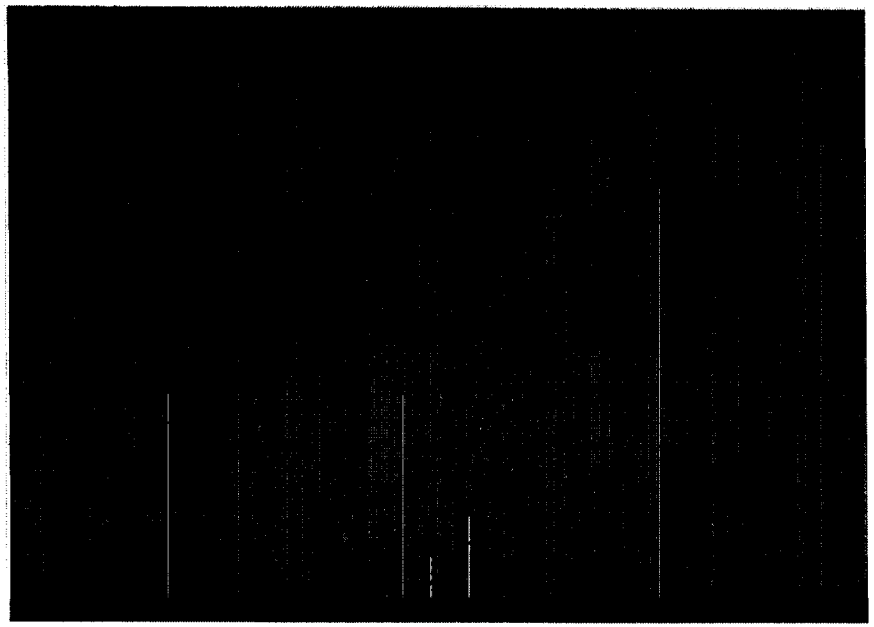

$V_{f_{porosity}}$=.09%

FIGURE 1. ALLOY 10 MICROSTRUCTURE.

FIGURE 2. NOTCH FATIGUE SPECIMEN.

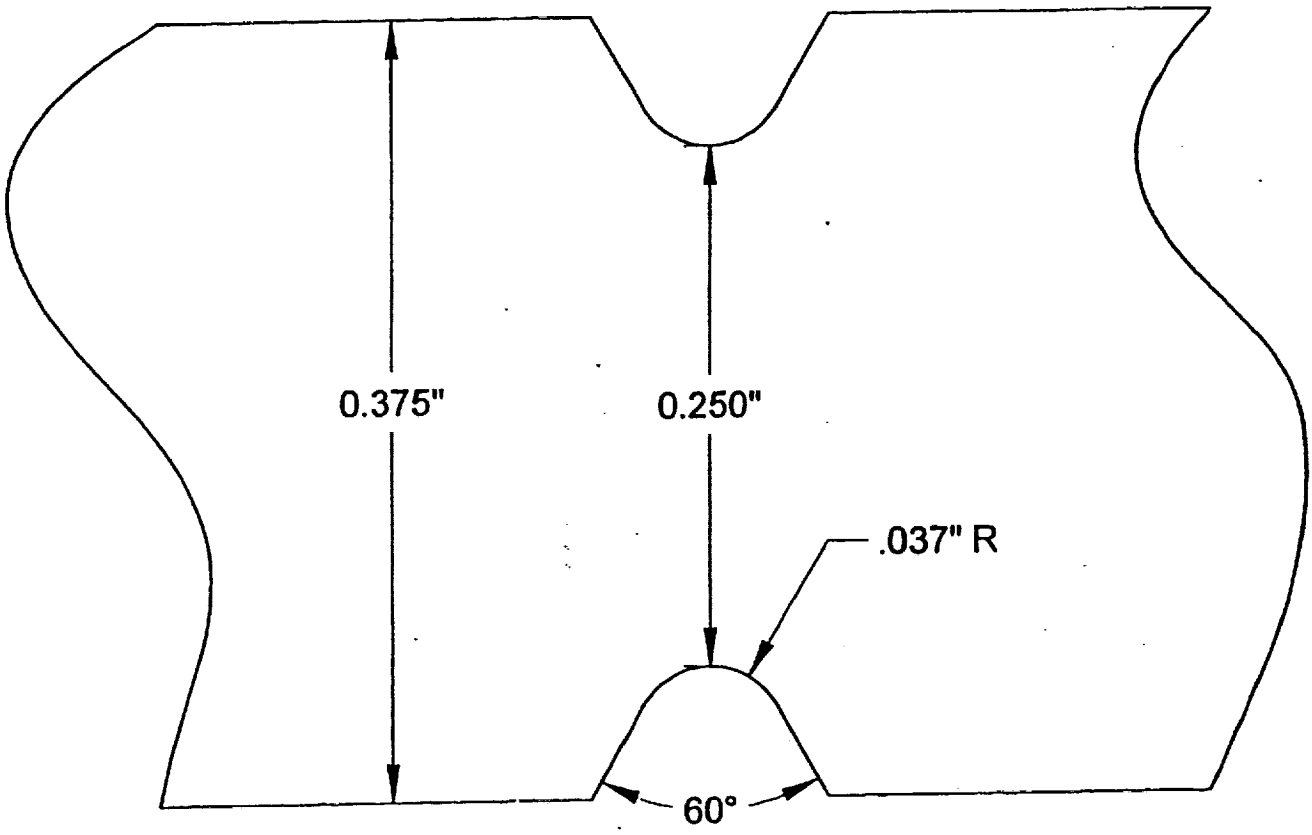

ROUND BAR (Kt=2)

FIGURE 3. MODULUS OF ALLOY 10.

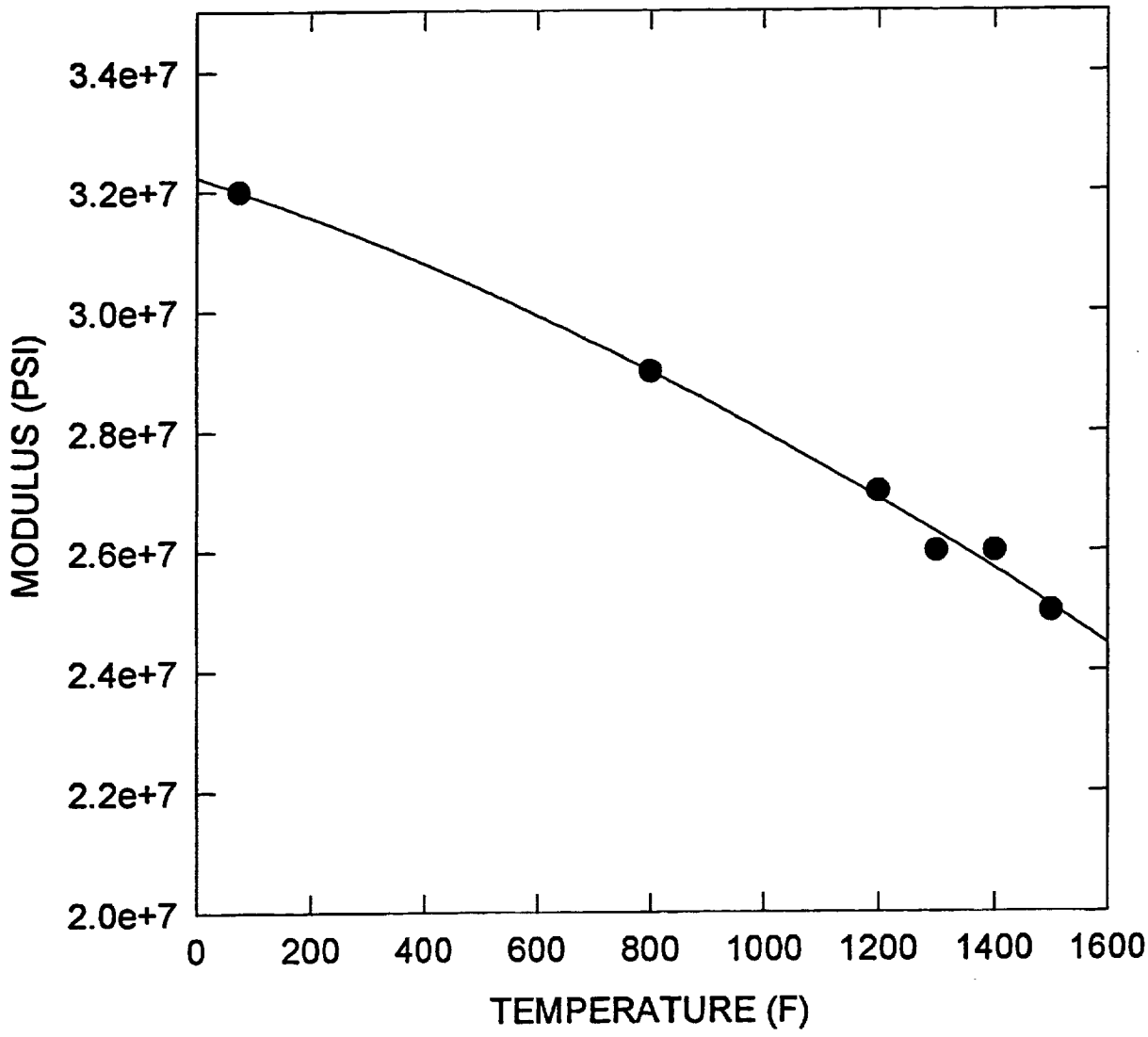

FIGURE 4. TENSILE STRENGTH OF ALLOY 10.

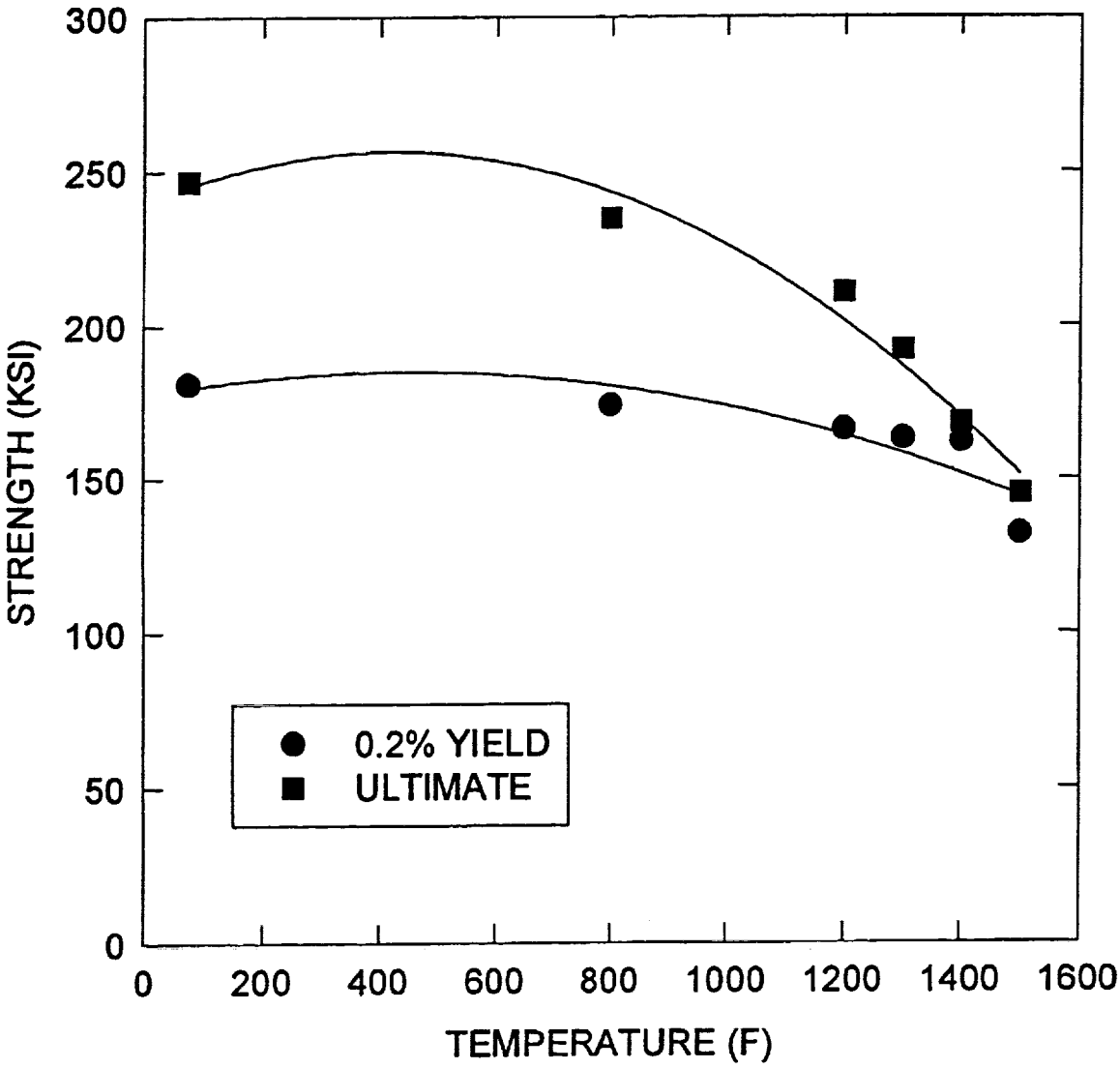

FIGURE 5. ELONGATION OF ALLOY 10.

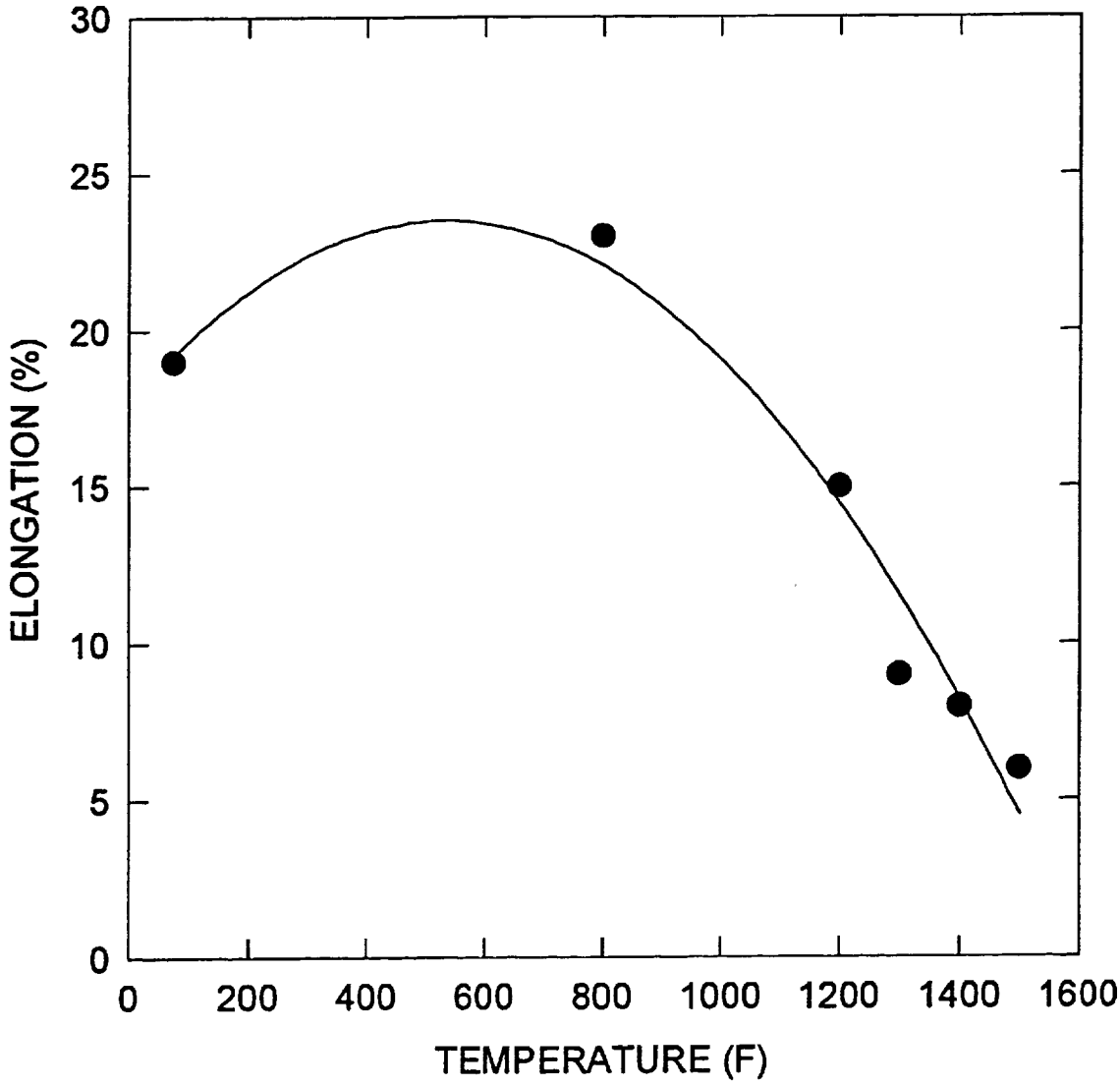

FIGURE 6. CREEP DATA OF ALLOY 10.

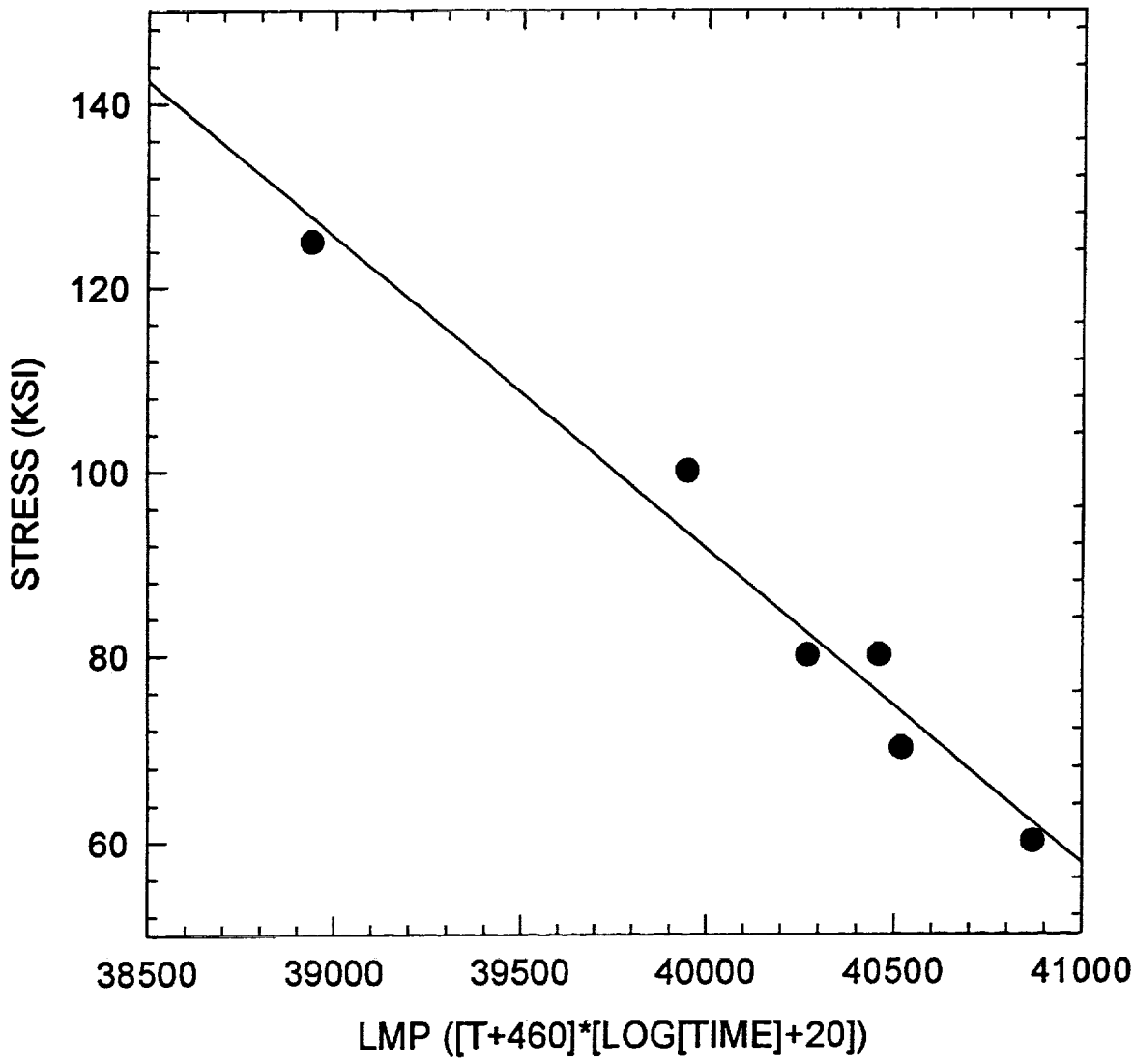

FIGURE 7. ALLOY 10 CRACK GROWTH DATA.

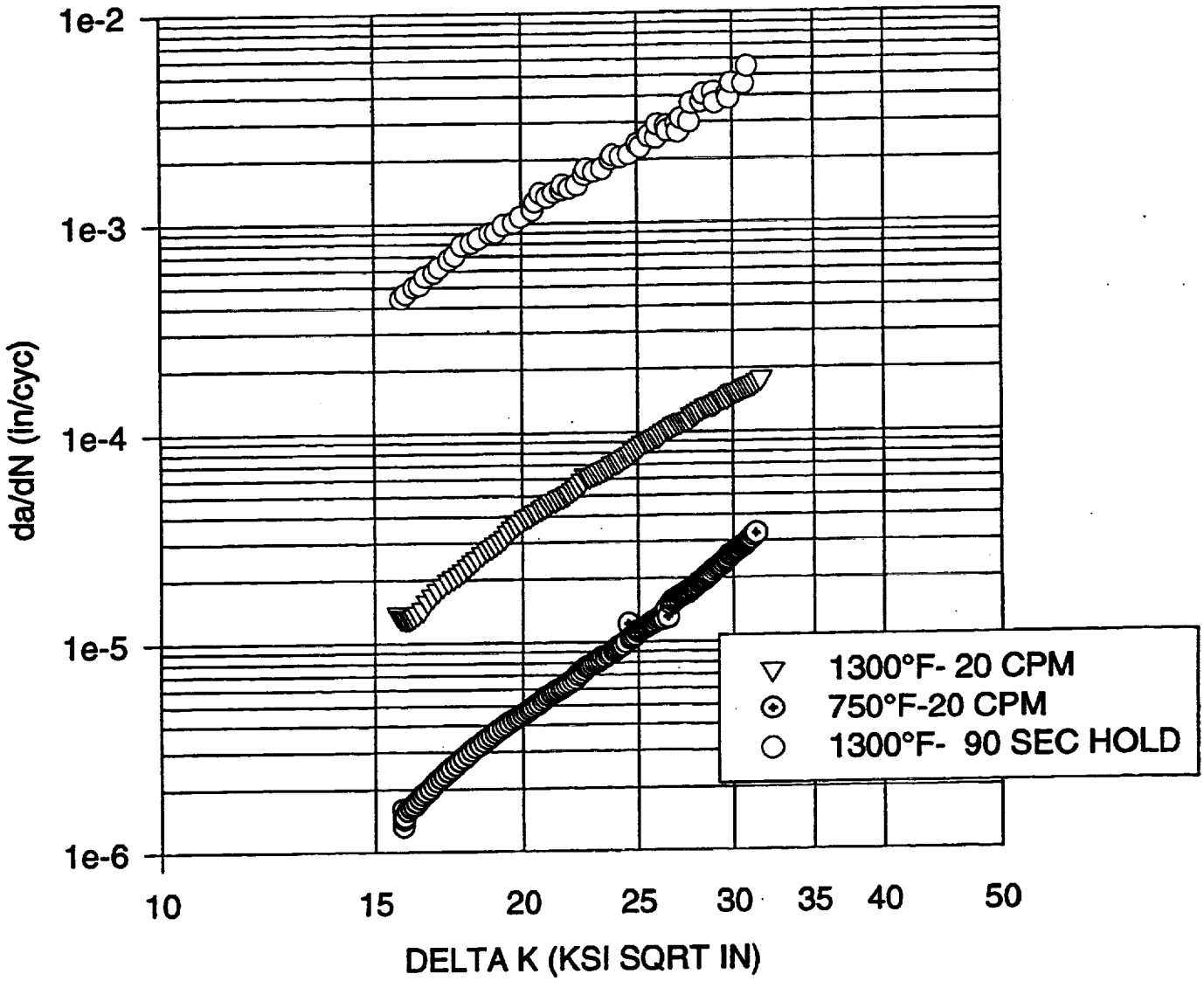

FIGURE 8. CYCLIC STRESS-STRAIN DATA AT 750F.

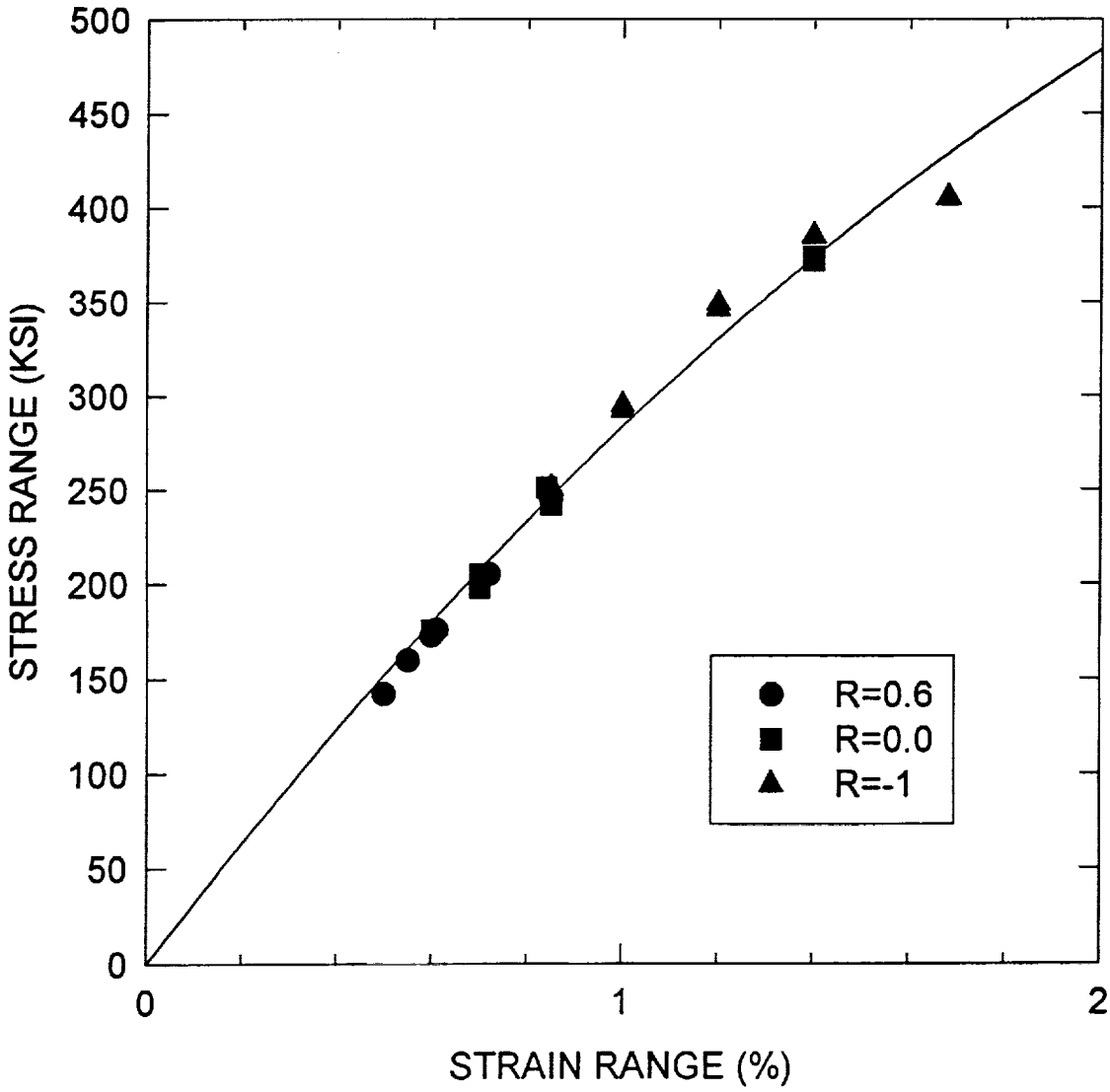

FIGURE 9. CYCLIC STRESS-STRAIN DATA AT 1300F.

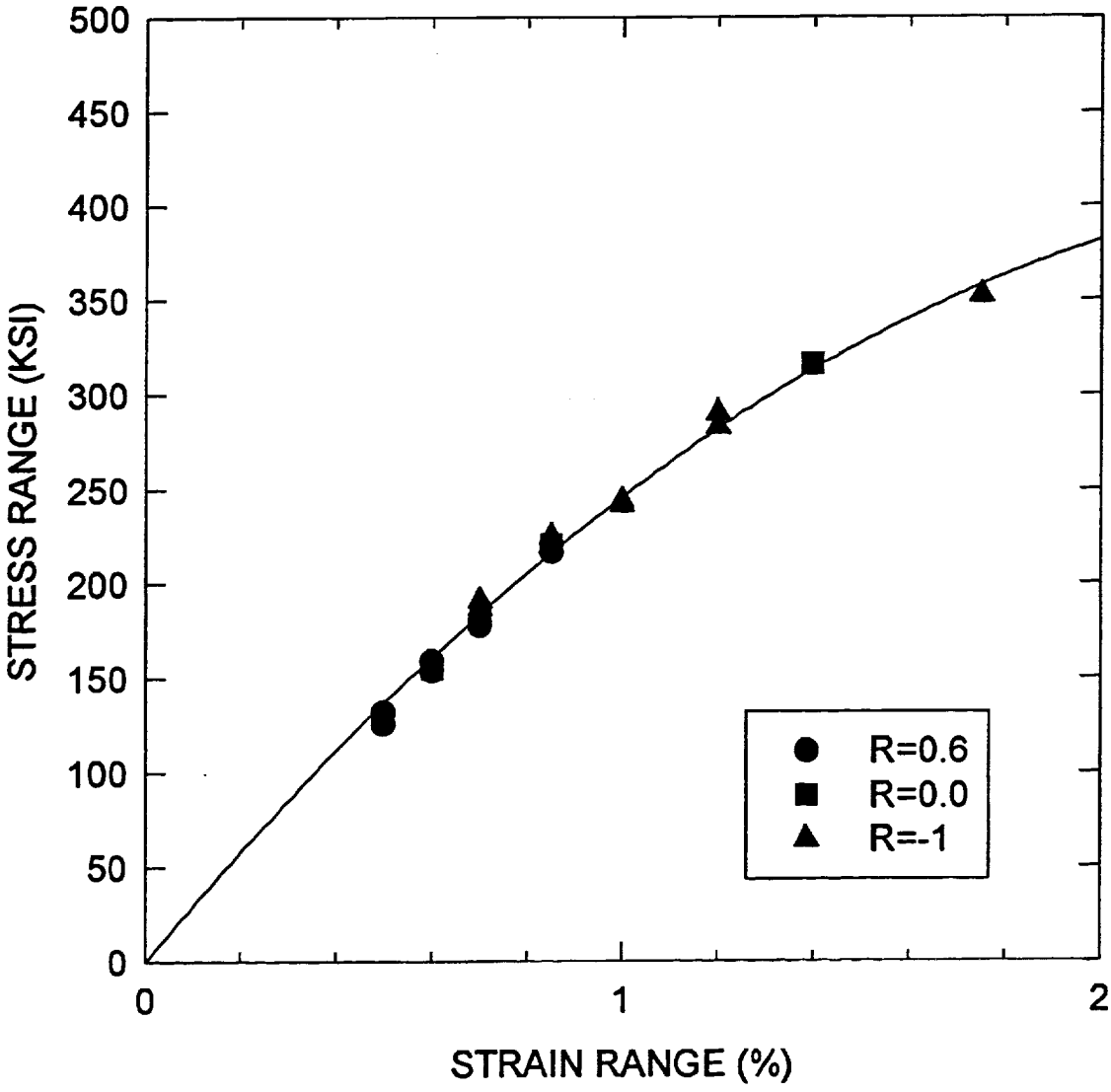

FIGURE 10. STRAIN RANGE VERSUS MAX STRESS AT 750F.

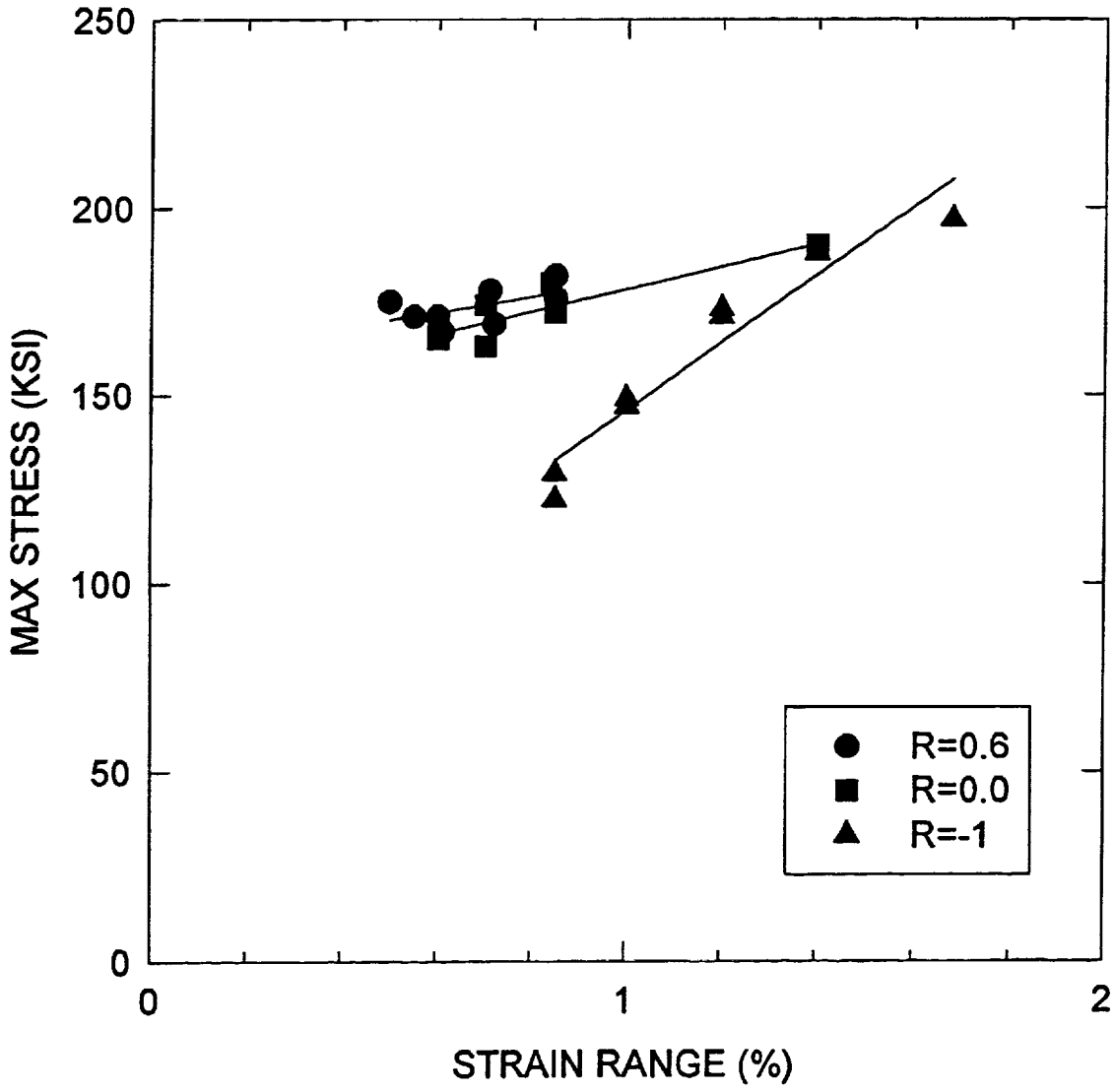

FIGURE 11. STRAIN RANGE VERSUS MAX STRESS AT 1300F.

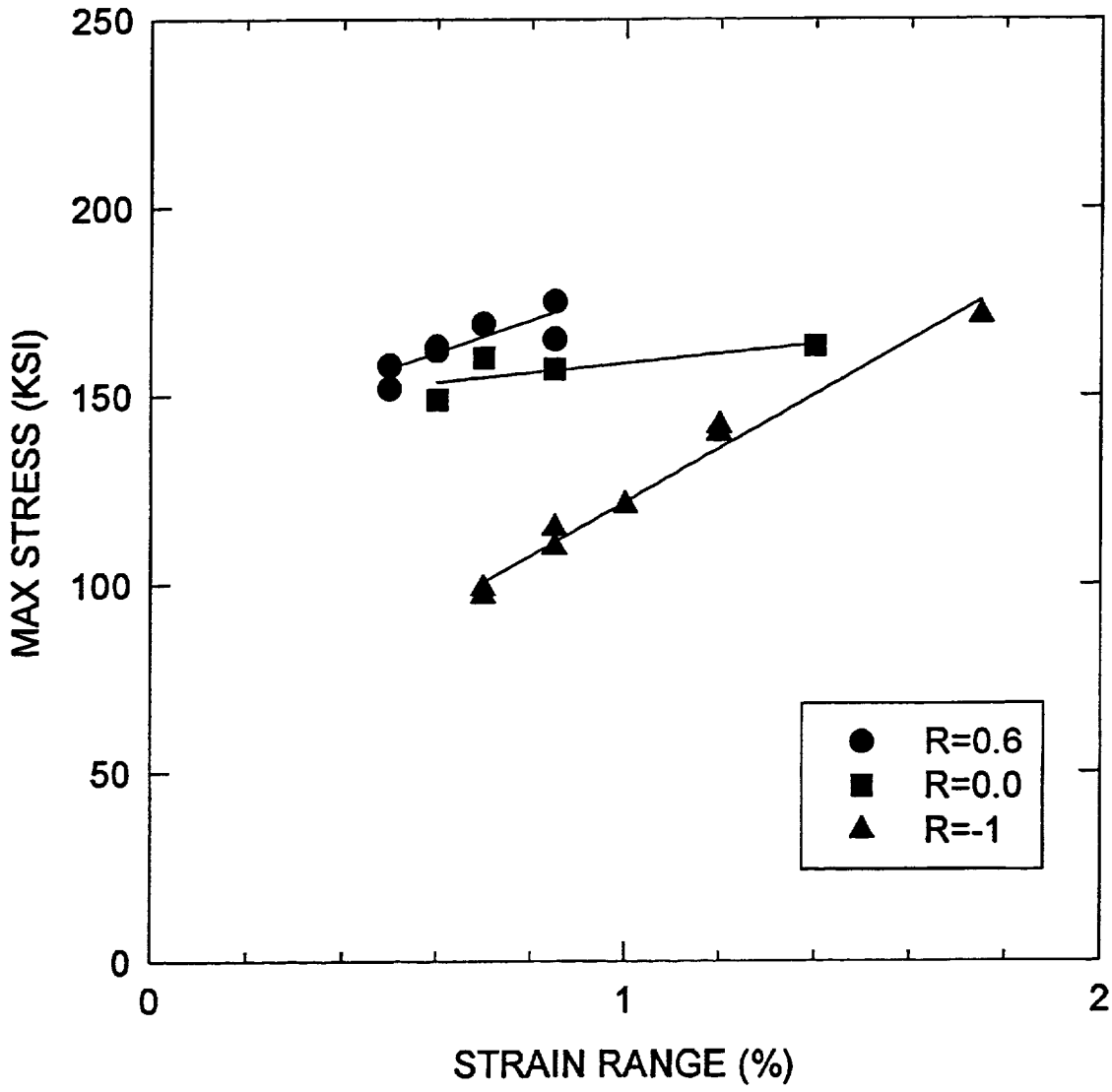

FIGURE 12. FATIGUE DATA AT 750F.

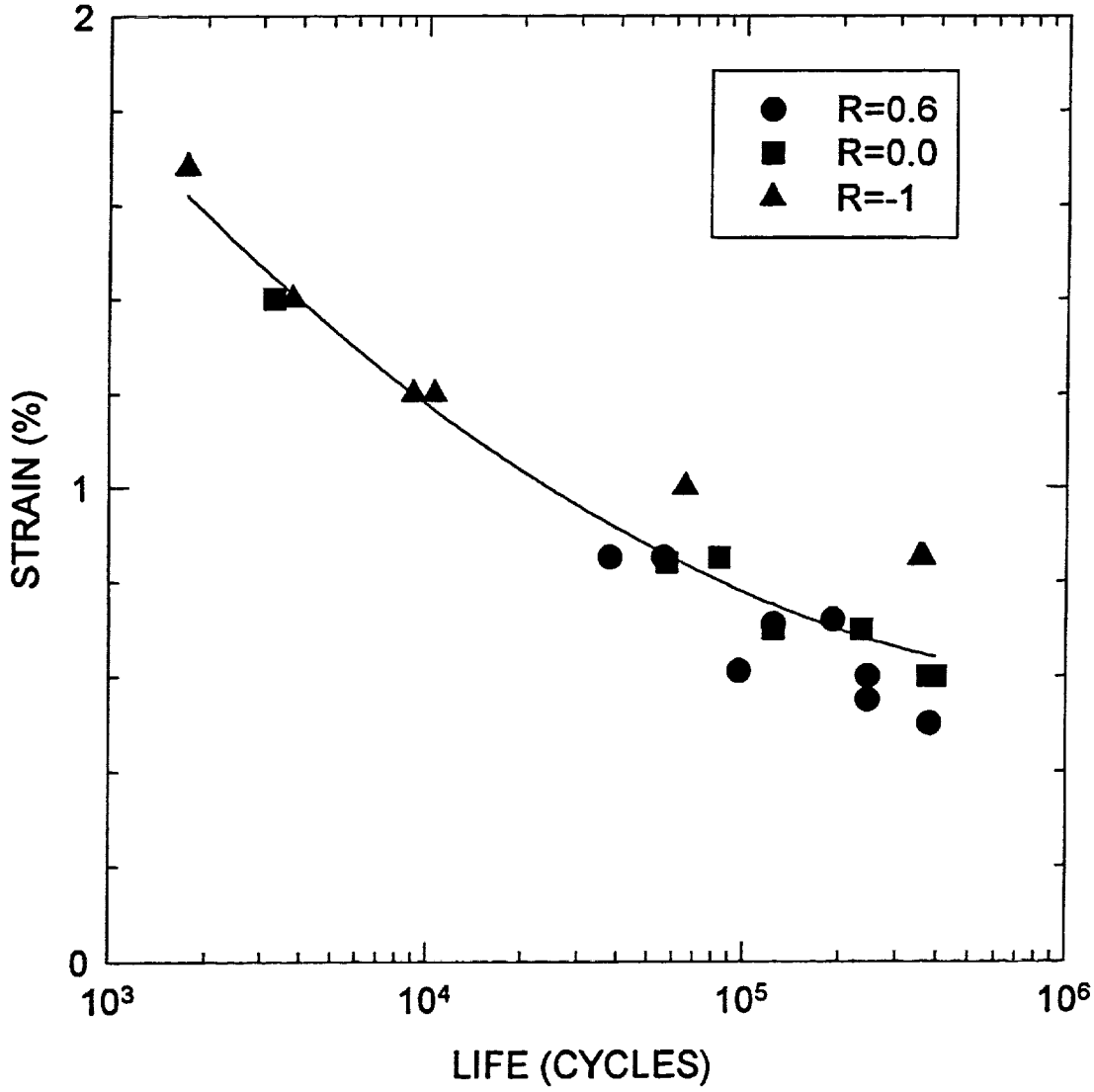

FIGURE 13. FATIGUE DATA AT 1300F.

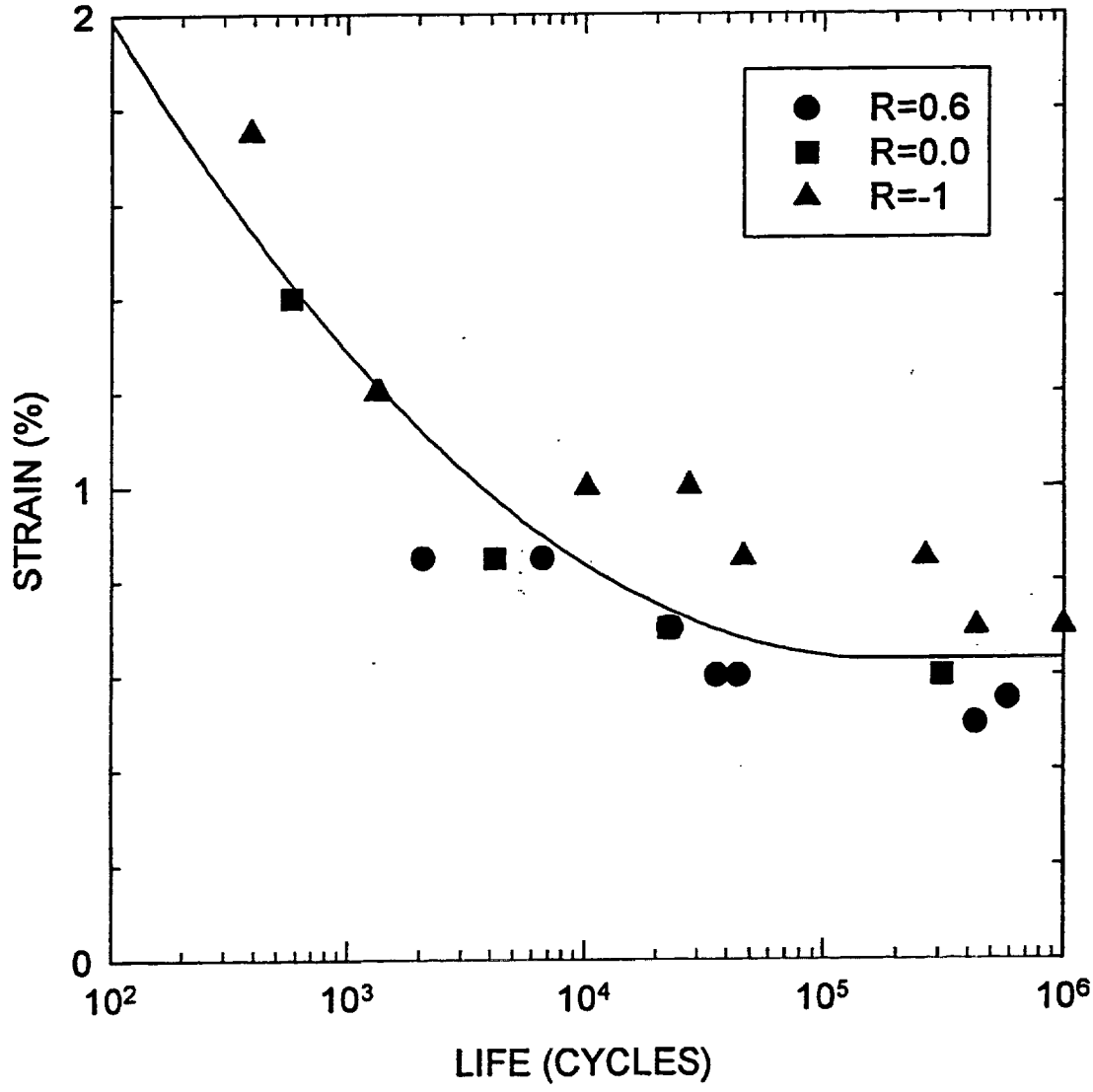

FIGURE 14. SMITH-WATSON-TOPPER FATIGUE PLOT AT 750F.

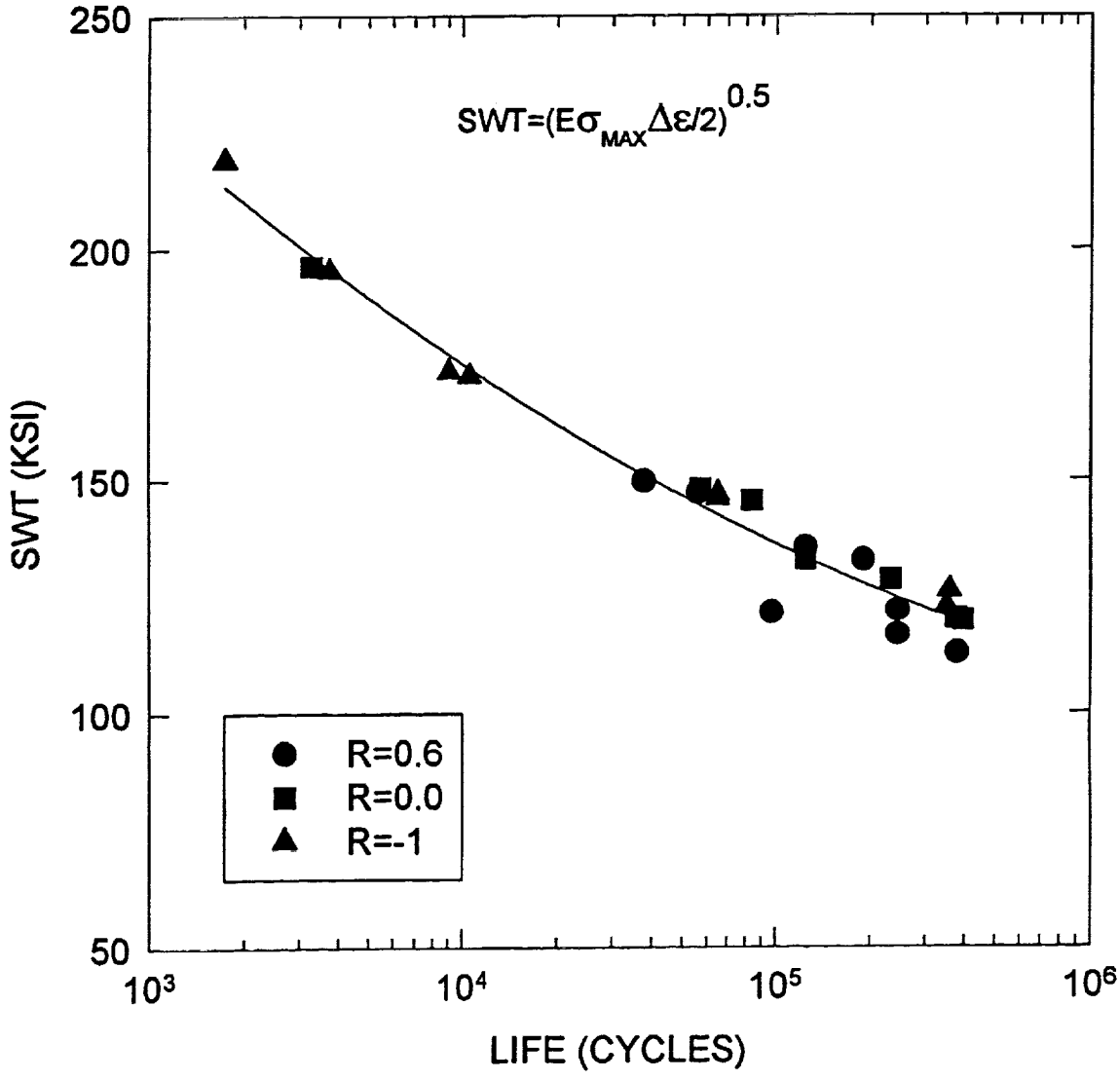

FIGURE 15. SMITH-WATSON-TOPPER FATIGUE PLOT AT 1300F.

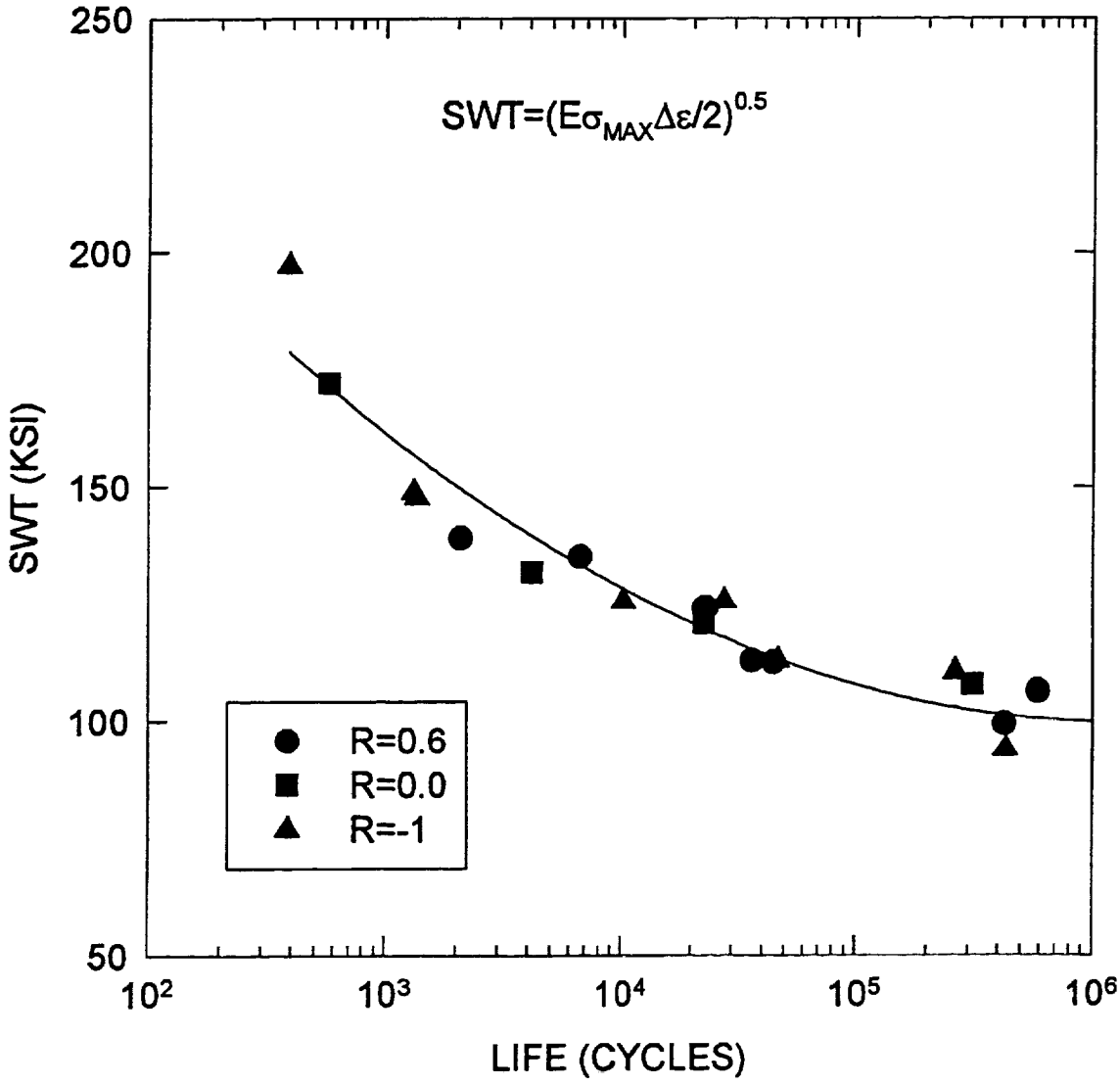

FIGURE 16. EFFECT OF TEMPERATURE ON FATIGUE LIFE.

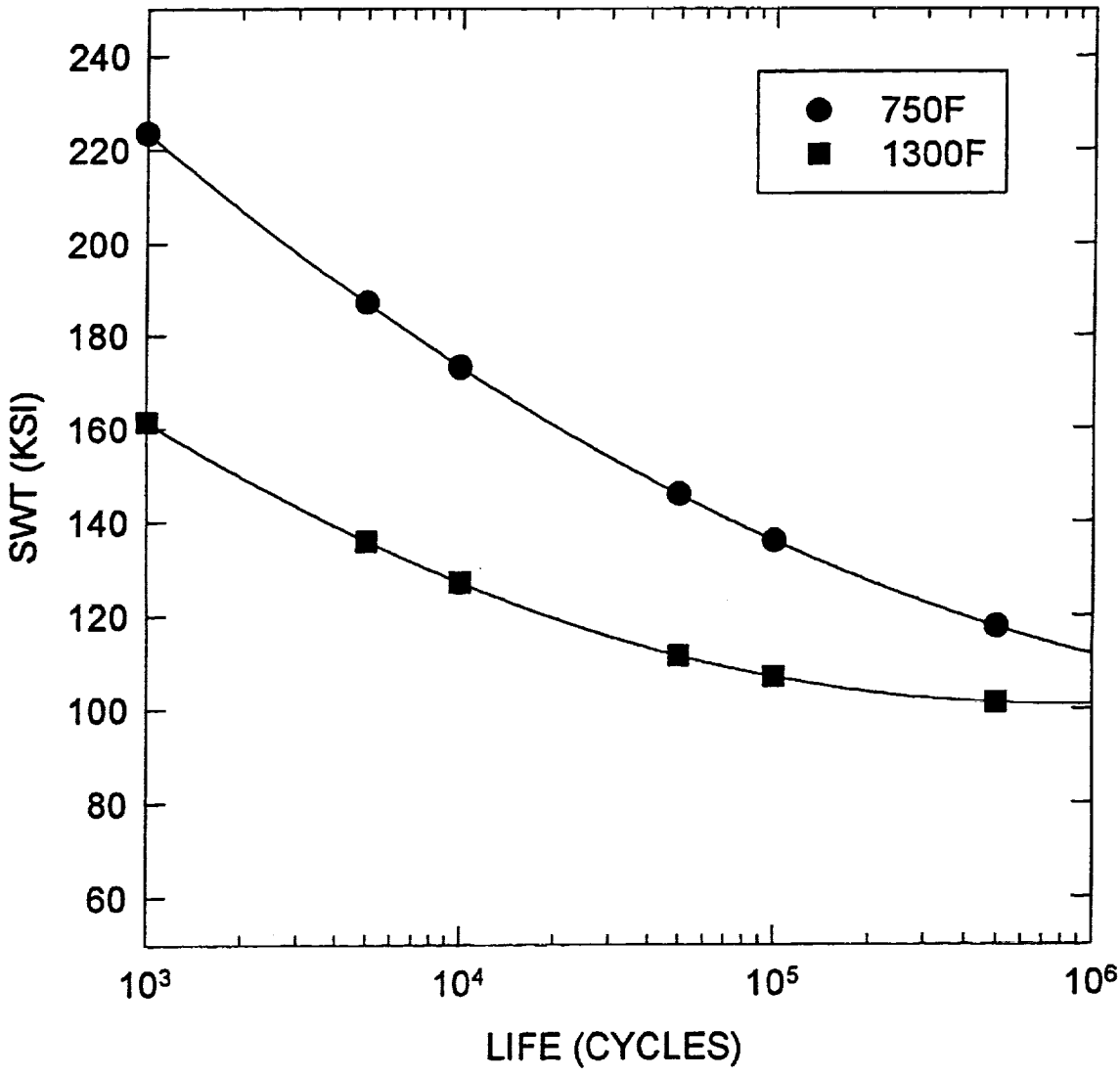

FIGURE 17. NOTCH FATIGUE DATA AT 750F.

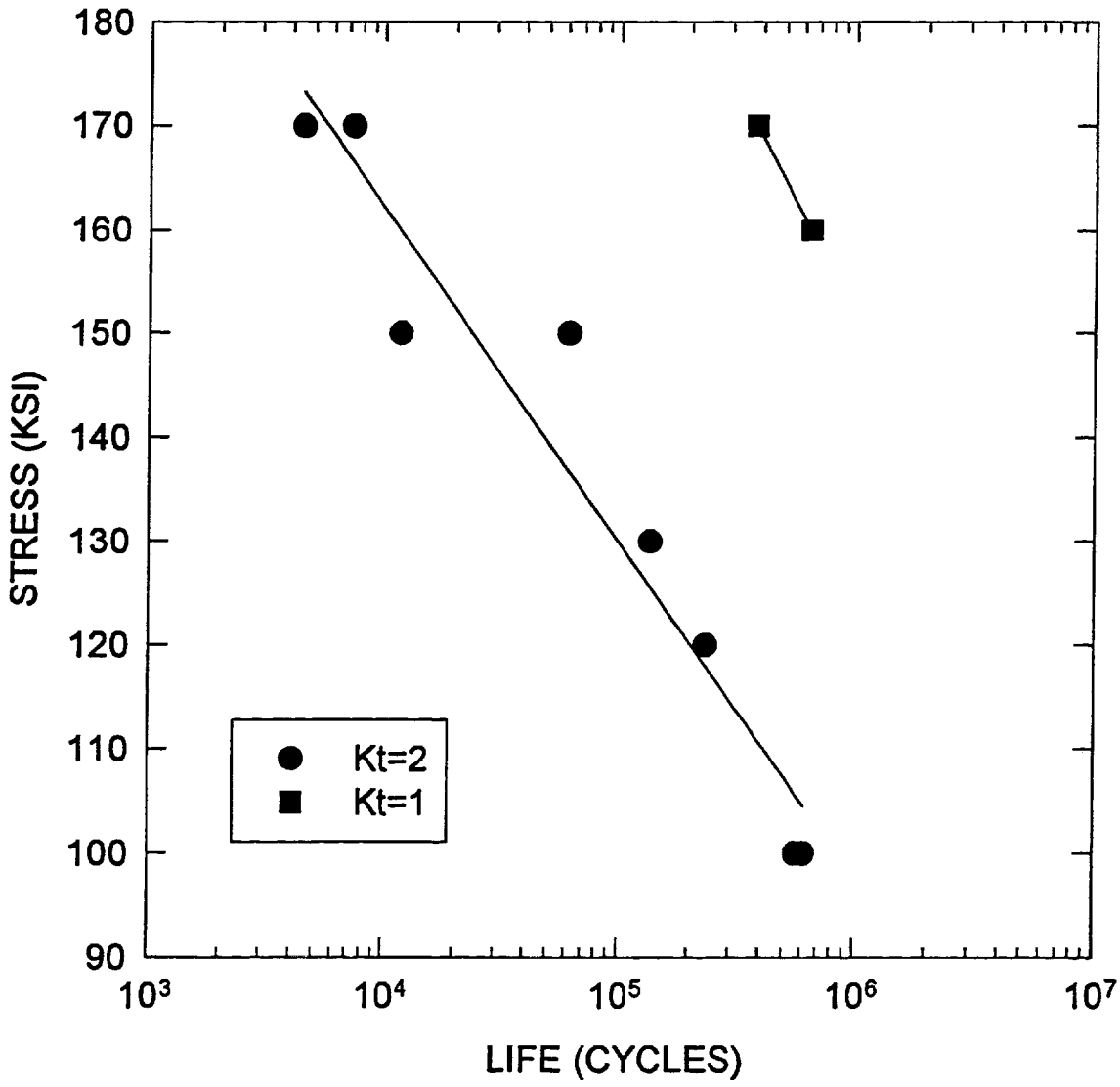

FIGURE 18. NOTCH FATIGUE DATA AT 1300F.

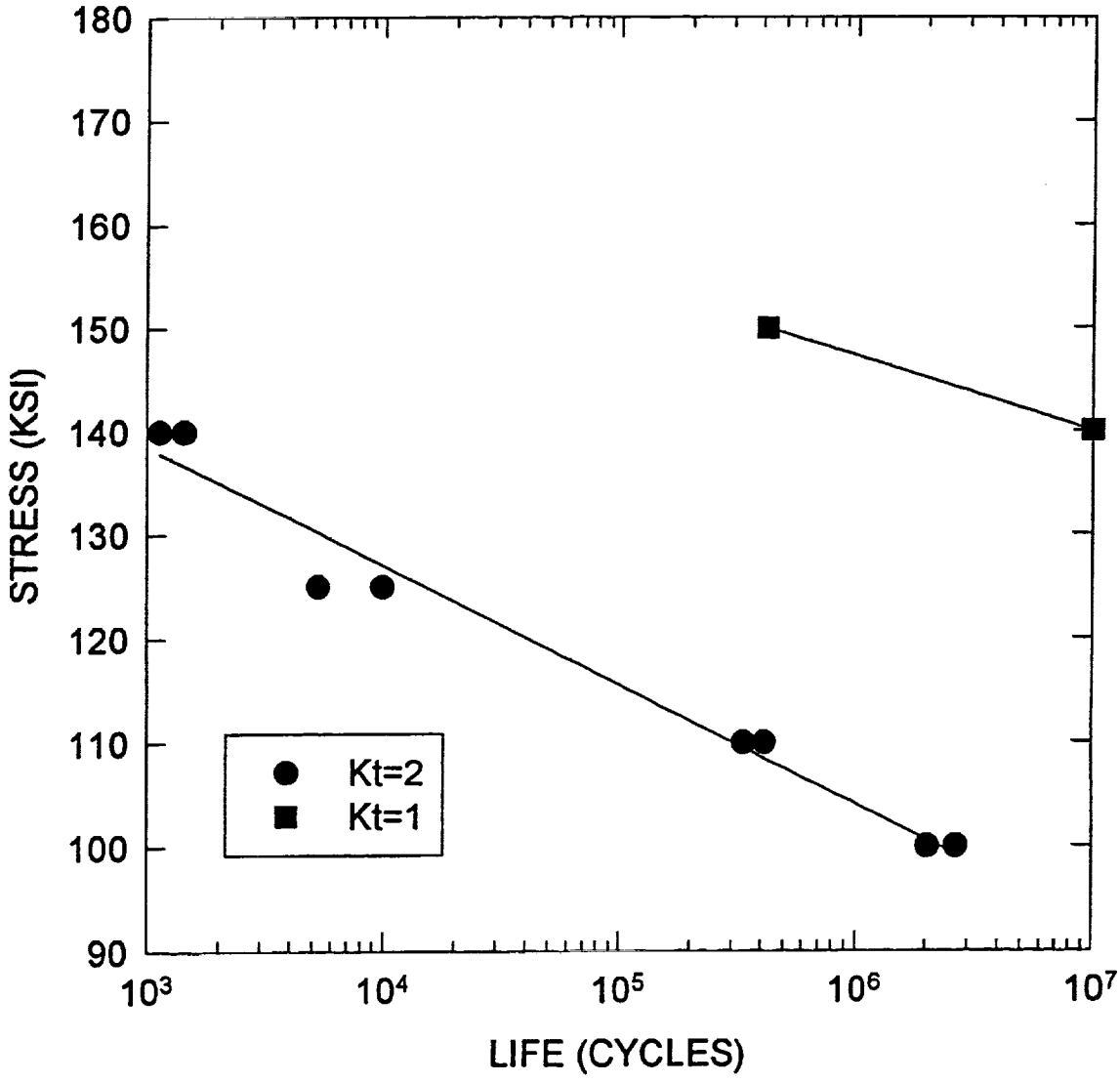

FIGURE 19. NOTCH FATIGUE DATA (Kt=2).

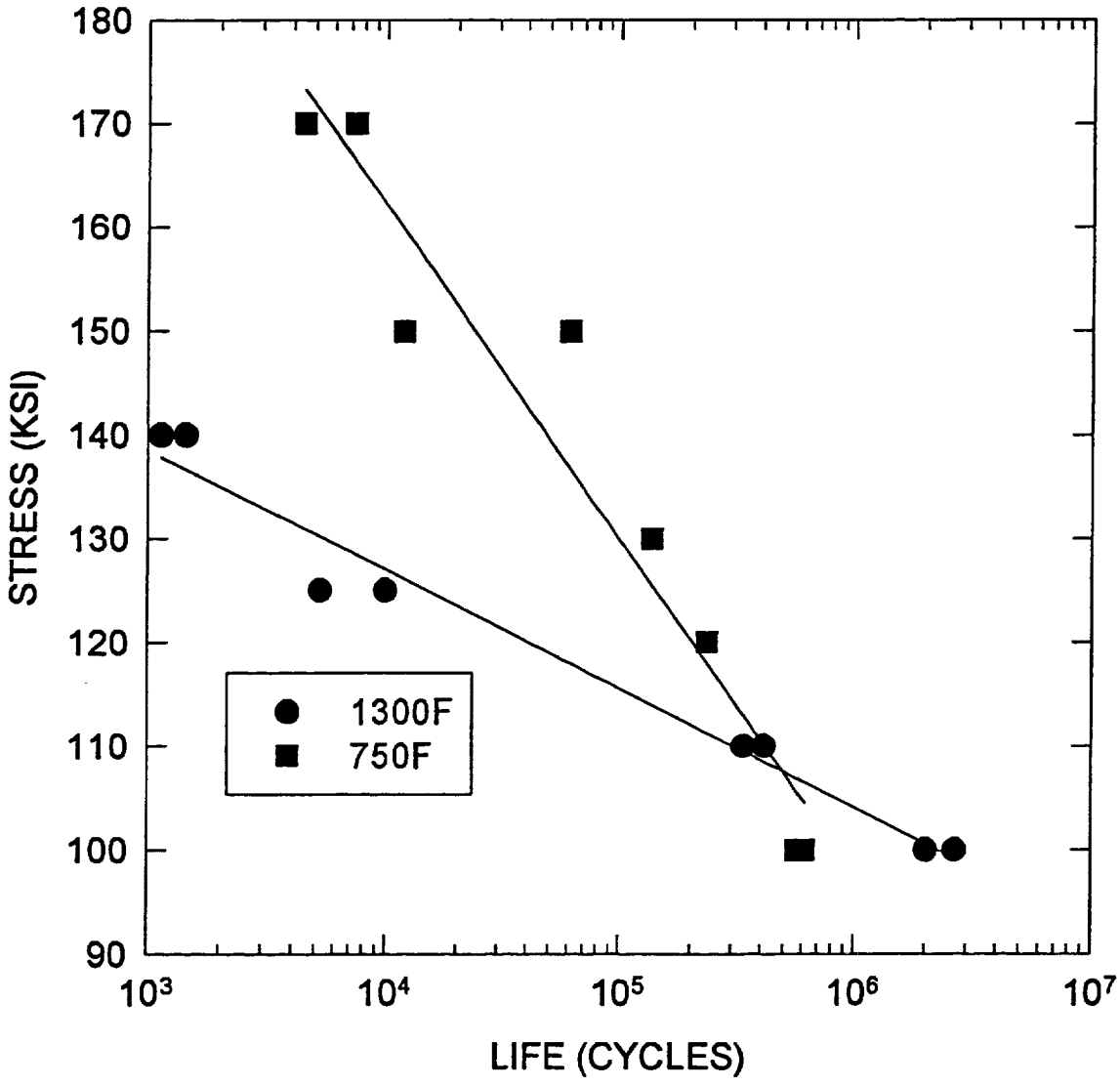

FIGURE 20. 1300F RELAXATION RATE FOR ALLOY 10.

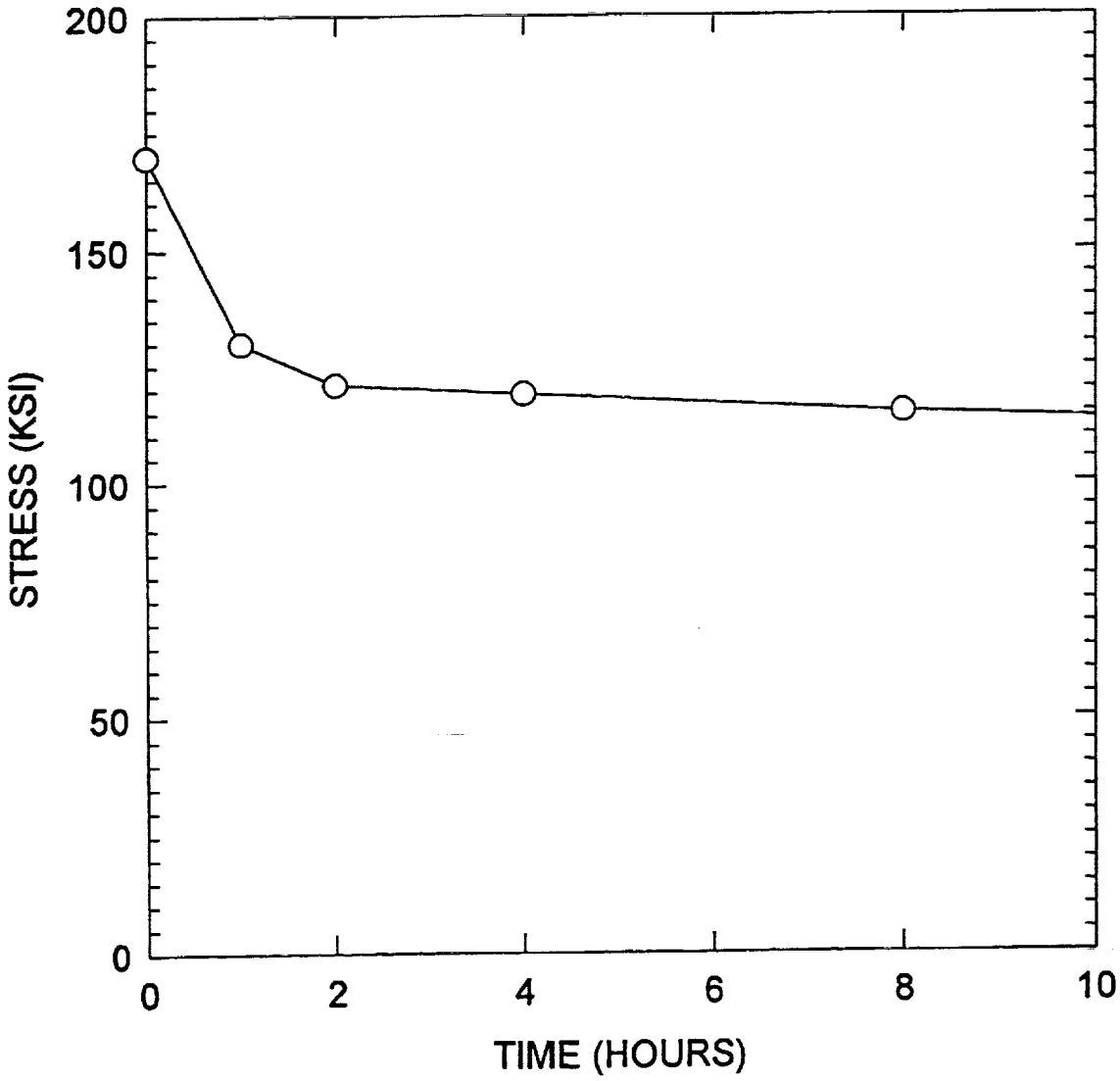

FIGURE 21. AXIAL STRESS DISTRIBUTION AT PEAK LOAD.

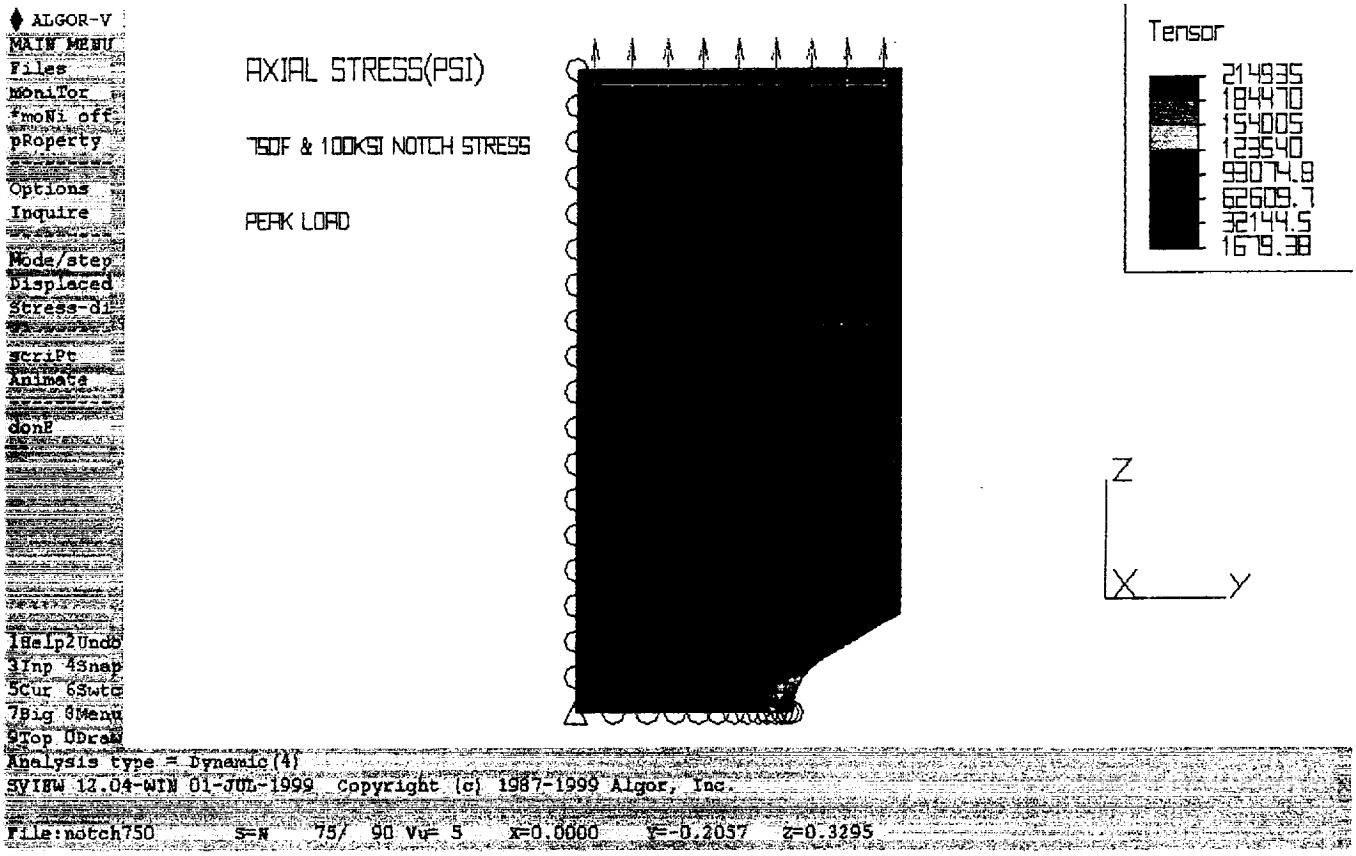

FIGURE 22. AXIAL STRESS DISTRIBUTION AT ZERO LOAD.

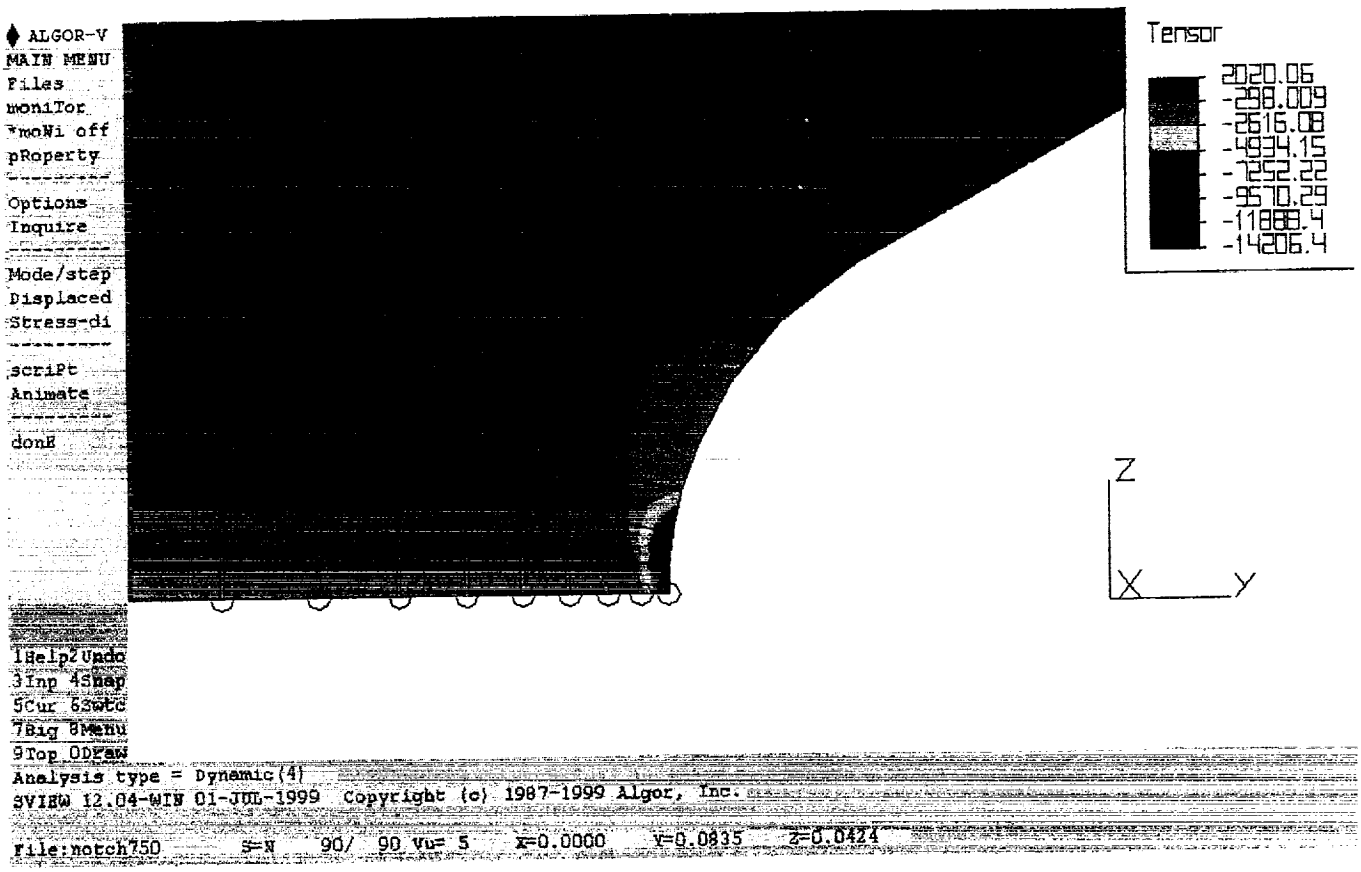

FIGURE 23. LOADING FUNCTION FOR STRESS ANALYSIS.

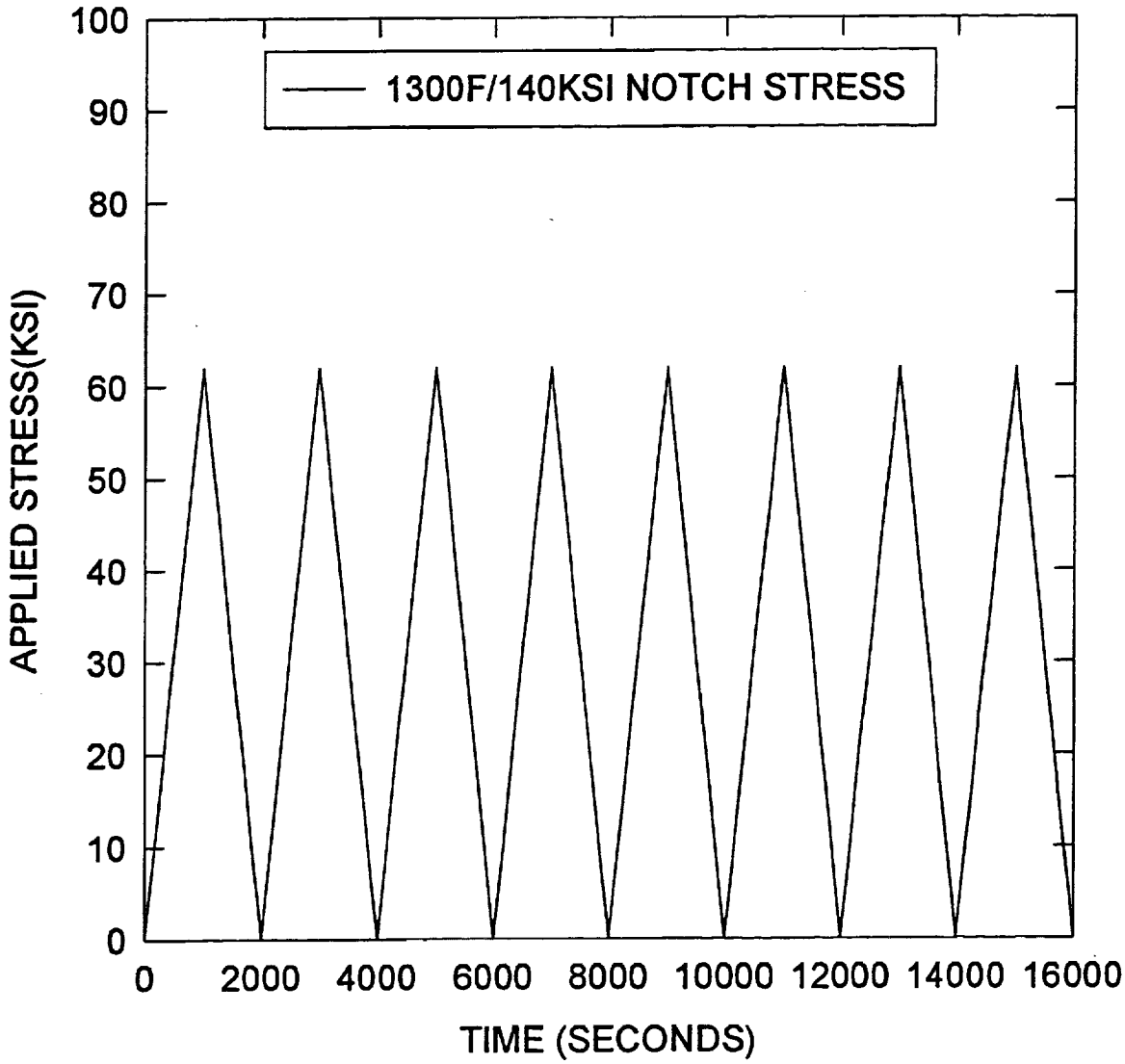

FIGURE 24. EVOLUTION OF PEAK STRESS AT NOTCH ROOT.

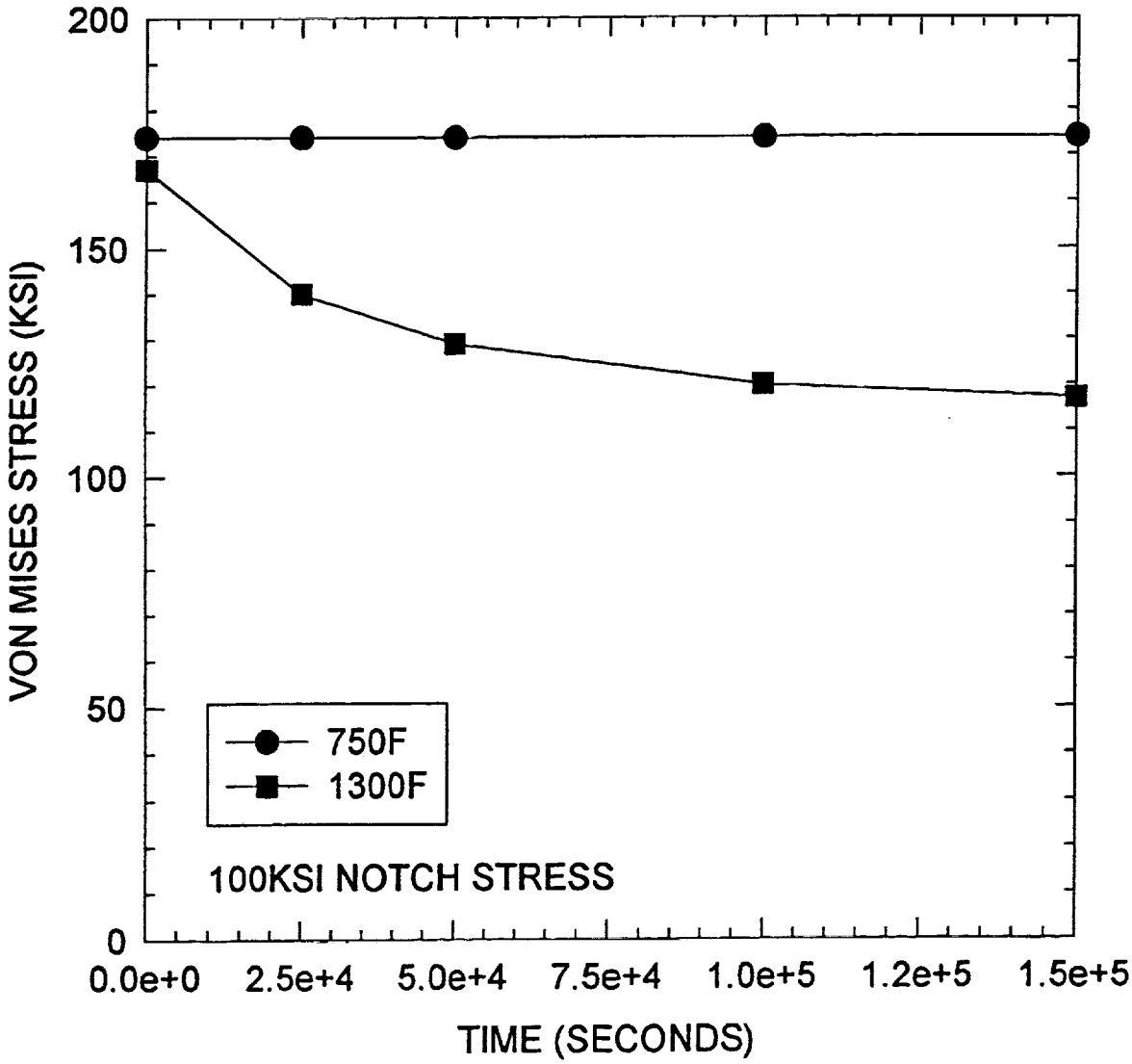

FIGURE 25. EVOLUTION OF PEAK STRESS AT NOTCH ROOT.

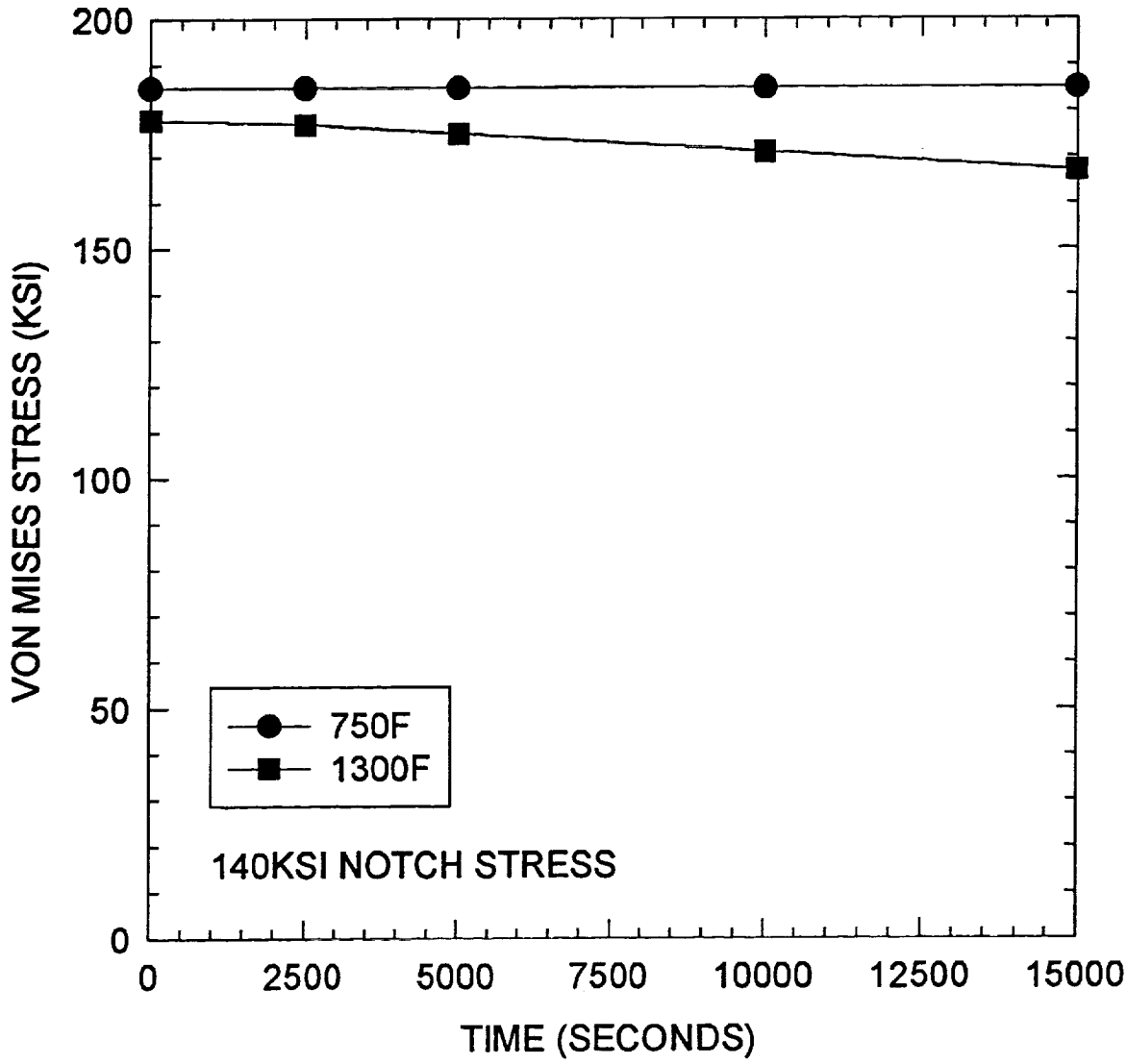

FIGURE 26. NOTCH FATIGUE PREDICTIONS.

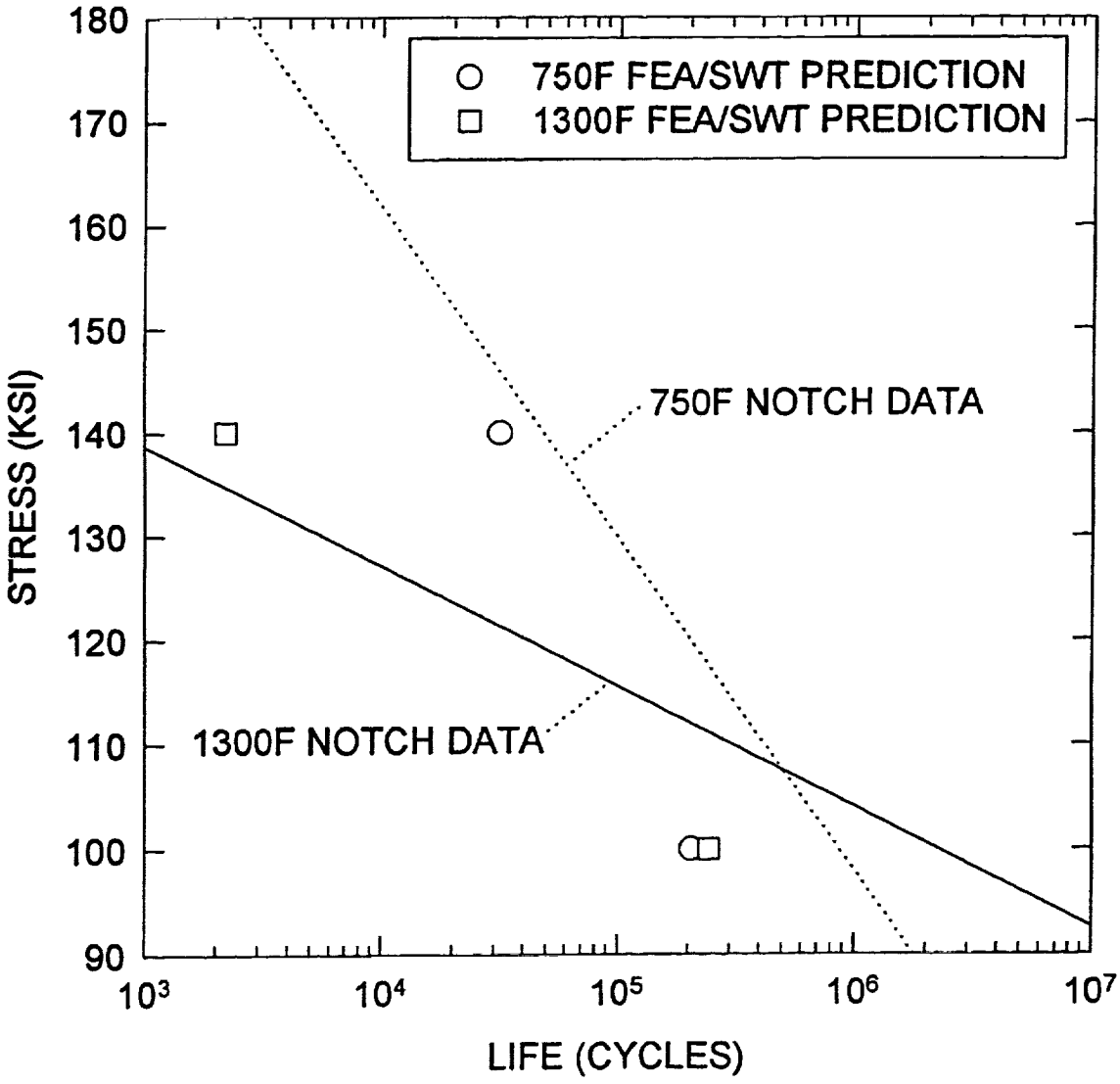

APPENDIX

	750F/100KSI					750F/140KSI			
TIME	EFF STRESS	EFF STRAIN	AXIAL STRESS	AXIAL STRAIN	TIME	EFF STRESS	EFF STRAIN	AXIAL STRESS	AXIAL STRAIN
(SEC)	(KSI)	(%)	(KSI)	(%)	(SEC)	(KSI)	(%)	(KSI)	(%)
0.00	0	0.00	0	0.00	0.00	0	0.00	0	0.00
1.50	174	0.66	215	0.73	1.50	185	1.18	241	1.19
3.00	22	0.03	-14	0.03	3.00	90	0.31	-74	0.22
4.50	174	0.67	215	0.74	4.50	185	1.18	241	1.19
6.00	22	0.03	-14	0.03	6.00	90	0.31	-74	0.22
7.50	174	0.67	215	0.74	7.50	185	1.18	241	1.19
9.00	22	0.03	-14	0.03	9.00	90	0.31	-74	0.22

				STABILIZED STRESSES AND STRAINS								
TIME	TEMP	Snotch	Sx	Sy	Sz	Tyz	Svm	Ex	Ey	Ez	Eyz	Evm
(SEC)	(F)	(KSI)	(KSI)	(KSI)	(KSI)	(KSI)	(KSI)	(%)	(%)	(%)	(%)	(%)
5000	750	140	101	31	241	3	185	0.05	-0.60	1.19	0.02	1.59
5000	750	0	17	14	-74	2	90	0.00	-0.27	0.22	0.02	0.42
150000	750	100	69	22	215	2	174	-0.03	-0.27	0.74	0.00	0.91
150000	750	0	7	9	-14	0	22	0.00	-0.03	0.03	0.00	0.05
		NOTE:EFFECTIVE STRAIN=Evm/1.35.										

	1300F/100KSI					1300F/140KSI			
TIME	EFF STRESS	EFF STRAIN	AXIAL STRESS	AXIAL STRAIN	TIME	EFF STRESS	EFF STRAIN	AXIAL STRESS	AXIAL STRAIN
(SEC)	(KSI)	(%)	(KSI)	(%)	(SEC)	(KSI)	(%)	(KSI)	(%)
0.00	0	0.00	0	0.00	0.00	0	0.00	0	0.00
1.50	167	0.80	208	0.85	1.50	178	1.39	240	1.39
3.00	35	0.10	-24	0.07	3.00	99	0.43	-84	0.30
10000	158	0.82	206	0.88	1000	178	1.39	240	1.39
20000	51	0.19	-40	0.13	2000	99	0.44	-84	0.31
30000	139	0.94	185	0.97	3000	177	1.41	240	1.40
40000	65	0.28	-53	0.20	4000	100	0.45	-85	0.32
50000	129	1.03	176	1.03	5000	175	1.43	238	1.42
60000	72	0.36	-60	0.26	6000	102	0.48	-87	0.35
70000	125	1.08	171	1.07	7000	173	1.47	236	1.45
80000	76	0.41	-64	0.30	8000	104	0.52	-89	0.37
90000	122	1.13	169	1.11	9000	171	1.50	234	1.47
100000	79	0.45	-67	0.33	10000	106	0.55	-91	0.40
110000	119	1.17	167	1.14	11000	170	1.53	233	1.50
120000	81	0.49	-68	0.36	12000	108	0.58	-92	0.42
130000	118	1.21	165	1.17	13000	169	1.55	231	1.52
140000	82	0.52	-70	0.39	14000	109	0.60	-93	0.44
150000	117	1.24	164	1.20	15000	167	1.57	230	1.54

STABILIZED STRESSES AND STRAINS												
TIME	TEMP	Snotch	Sx	Sy	Sz	Tyz	Svm	Ex	Ey	Ez	Eyz	Evm
(SEC)	(F)	(KSI)	(KSI)	(KSI)	(KSI)	(KSI)	(KSI)	(%)	(%)	(%)	(%)	(%)
5000	1300	140	107	39	238	1	175	***	-0.78	1.42	0.02	1.93
5000	1300	0	16	14	-86	1	101	***	-0.40	0.34	0.02	0.64
150000	1300	100	78	32	164	1	117	***	-0.71	1.20	0.01	1.67
150000	1300	0	12	14	-71	1	83	***	-0.43	0.41	0.02	0.72
		NOTE:EFFECTIVE STRAIN=Evm/1.35 & Ex SHOULD BE NEAR ZERO BASED ON 750F ANALYSIS.										

REPORT DOCUMENTATION PAGE

Form Approved
OMB No. 0704-0188

Public reporting burden for this collection of information is estimated to average 1 hour per response, including the time for reviewing instructions, searching existing data sources, gathering and maintaining the data needed, and completing and reviewing the collection of information. Send comments regarding this burden estimate or any other aspect of this collection of information, including suggestions for reducing this burden, to Washington Headquarters Services, Directorate for Information Operations and Reports, 1215 Jefferson Davis Highway, Suite 1204, Arlington, VA 22202-4302, and to the Office of Management and Budget, Paperwork Reduction Project (0704-0188), Washington, DC 20503.

1. AGENCY USE ONLY (*Leave blank*)	2. REPORT DATE	3. REPORT TYPE AND DATES COVERED
	November 2000	Technical Memorandum

4. TITLE AND SUBTITLE

Fatigue Characterization of Alloy 10: A 1300F Disk Alloy for Small Gas Turbine Engines

5. FUNDING NUMBERS

WU–708–24–13–00

6. AUTHOR(S)

John Gayda

7. PERFORMING ORGANIZATION NAME(S) AND ADDRESS(ES)

National Aeronautics and Space Administration
John H. Glenn Research Center at Lewis Field
Cleveland, Ohio 44135–3191

8. PERFORMING ORGANIZATION REPORT NUMBER

E–12543

9. SPONSORING/MONITORING AGENCY NAME(S) AND ADDRESS(ES)

National Aeronautics and Space Administration
Washington, DC 20546–0001

10. SPONSORING/MONITORING AGENCY REPORT NUMBER

NASA TM—2000-210576

11. SUPPLEMENTARY NOTES

Responsible person, John Gayda, organization code 5120, 216–433–3273.

12a. DISTRIBUTION/AVAILABILITY STATEMENT

Unclassified - Unlimited
Subject Category: 26 Distribution: Nonstandard

Available electronically at http://gltrs.grc.nasa.gov/GLTRS
This publication is available from the NASA Center for AeroSpace Information, 301–621–0390.

12b. DISTRIBUTION CODE

13. ABSTRACT ***(Maximum 200 words)***

A detailed fatigue characterization of Alloy 10, a high strength nickel-based disk alloy, was conducted on test coupons machined from a "pancake" forging. Smooth bar, strain controlled fatigue testing at various R-ratios was run at representative bore, 750F, and rim, 1300F, temperatures. This was followed by notch fatigue testing (Kt=2) run under load control. Analysis of the fatigue data using a Smith-Watson-Topper approach and finite element analysis of the notch root was employed to understand material behavior in these tests. Smooth bar fatigue data showed a significant R-ratio dependence at either test temperature which could be accounted for using a Smith-Watson-Topper parameter, SWT. In general, fatigue life was longer at 750F than 1300F for a given SWT. For notch fatigue tests, life was longer at 750F than 1300F but only at higher stresses. This was attributed to differences in alloy strength. At lower stresses, finite element analysis suggested that convergence of fatigue life at both temperatures resulted from relaxation of stresses at the notch root in the 1300F tests.

14. SUBJECT TERMS

Superalloy fatigue

15. NUMBER OF PAGES

43

16. PRICE CODE

A03

17. SECURITY CLASSIFICATION OF REPORT	18. SECURITY CLASSIFICATION OF THIS PAGE	19. SECURITY CLASSIFICATION OF ABSTRACT	20. LIMITATION OF ABSTRACT
Unclassified	Unclassified	Unclassified	